

Segmental patterns of vestibular-mediated synaptic inputs to axial and limb motoneurons in the neonatal mouse assessed by optical recording

Nedim Kasumacic, Joel C. Glover and Marie-Claude Perreault

University of Oslo, Institute of Basic Medical Sciences (Domus Medica), Department of Physiology, N-0317 Oslo, Norway

Proper control of movement and posture occurs partly via descending projections from the vestibular nuclei to spinal motor circuits. Days before birth in rodents, vestibulospinal neurons develop axonal projections that extend to the spinal cord. How functional these projections are just after birth is unknown. Our goal was to assess the overall functional organization of vestibulospinal inputs to spinal motoneurons in a brainstem–spinal cord preparation of the neonatal mouse (postnatal day (P) 0–5). Using calcium imaging, we recorded responses evoked by electrical stimulation of the VIIIth nerve, in many motoneurons simultaneously throughout the spinal cord (C2, C6, T7, L2 and L5 segments), in the medial and lateral motor columns. Selective lesions in the brainstem and/or spinal cord distinguished which tracts contributed to the responses: those in the cervical cord originated primarily from the medial vestibulospinal tracts but with a substantial contribution from the lateral vestibulospinal tract; those in the thoracolumbar cord originated exclusively from the lateral vestibulospinal tract. In the thoracolumbar but not the cervical cord, excitatory commissural connections mediated vestibular responses in contralateral motoneurons. Pharmacological blockade of GABA_A receptors showed that responses involved a convergence of excitatory and inhibitory inputs which in combination produced temporal response patterns specific for different segmental levels. Our results show that by birth vestibulospinal projections in rodents have already established functional synapses and are organized to differentially regulate activity in neck and limb motoneurons in a tract- and segment-specific pattern similar to that in adult mammals. Thus, this particular set of descending projections develops several key features of connectivity appropriately at prenatal stages. We also present novel information about vestibulospinal inputs to axial motoneurons in mammals, providing a more comprehensive platform for future studies into the overall organization of vestibulospinal inputs and their role in regulating postural stability.

(Received 30 June 2010; accepted after revision 16 October 2010; first published online 20 October 2010)

Corresponding author M.-C. Perreault: University of Oslo, Institute of Basic Medical Sciences, Department of Physiology, Sognsvannsveien 9, PB 1103 Blindern, N-0317, Oslo, Norway. Email: m.c.perreault@basalmed.uio.no

Abbreviation aCSF, artificial cerebrospinal fluid; c, contralateral; C1, first cervical spinal segment; C2, second cervical spinal segment; C8, eighth cervical spinal segment; CGDA, calcium green dextran amine; cMVST, contralateral medial vestibulospinal tract; E, embryonic day; i, ipsilateral; ICR, imprinting control region; iMVST, ipsilateral medial vestibulospinal tract; L2, second lumbar spinal segment; L5, fifth lumbar spinal segment; LMC, lateral motor column; LVST, lateral vestibulospinal tract; MLF, medial longitudinal fasciculus; MMC, medial motor column; MN, motoneuron; Nkx6.2, NK6 homeobox 2; P, postnatal day; PTX, picrotoxin; RDA, rhodamine dextran amine; ROI, region of interest; T, current threshold; T7, seventh thoracic spinal segment; VF, ventral funiculus; VIIIth nerve, eighth cranial nerve; VLF, ventrolateral funiculus.

Introduction

Vestibulospinal projections play a key role in controlling movement and posture. Current knowledge about vestibulospinal connections in mammals is based mostly

on anatomical and electrophysiological studies in adults (Shapovalov *et al.* 1966; Lund & Pompeiano, 1968; Wilson & Yoshida, 1969; Grillner *et al.* 1970; Wilson *et al.* 1970; Hongo *et al.* 1971; Akaike *et al.* 1973; Shinoda *et al.* 2006). Vestibulospinal connections are mediated by axons

coursing in the ipsilaterally and contralaterally projecting components of the medial vestibulospinal tract (iMVST and cMVST, Glover & Petursdottir, 1988; Glover, 2000a; Pasqualetti *et al.* 2007) and lateral vestibulospinal tract (LVST) and innervate motoneurons (MNs) in distinct spinal segments. The MVST innervates MNs in cervical segments and mediates vestibulospinal reflexes controlling primarily neck muscles whereas the LVST innervates MNs in cervical and lumbar segments and mediates vestibulospinal reflexes controlling the limbs (see Wilson & Peterson, 1978; Wilson *et al.* 1995; Shinoda *et al.* 2006 for reviews).

Despite the substantial information that has accumulated over the last 40 years in adults, several aspects of vestibulospinal organization remain to be elucidated, including the relative contributions of the separate iMVST and cMVST components (Glover, 2000a; Díaz *et al.* 2003), the distribution of functional connections to ipsi- and contralateral spinal segments, the degree of overlap between MVST and LVST innervation in cervical segments, and the possibility of functional connections to axial MNs that innervate trunk muscles.

Indirect evidence from anatomical and behavioural studies in several species has suggested that developing bulbospinal axons connect to appropriate MNs already at an early stage of development (reviewed in Glover, 2000b). It is unclear, however, the extent to which adult functional connectivity patterns are established already in neonates. Thus, our goal here has been twofold: (1) to determine whether vestibulospinal projections have established functional synaptic connections in the neonatal mouse and (2) to assess more comprehensively the tract- and segment-specific pattern of vestibulospinal connections to MNs for a developmental comparison and with particular attention to some of the issues that have been difficult to address in the adult. To do this we have used an optical recording approach developed specifically to assess functional bulbospinal connections during early postnatal life (P0–5) in the mouse (Szokol *et al.* 2008; Szokol & Perreault, 2009).

The vestibulospinal system of the mouse is well suited for this approach since the projections that constitute the vestibulospinal reflex pathway already develop anatomically during embryonic life. Vestibular sensory neurons become postmitotic between embryonic day (E) 10 and E12 (Ruben, 1967), send their peripheral axons into the otocyst at around E12 (Sher, 1971), make their first contacts with peripheral hair cells by E14 (see, however, Van de Water *et al.* 1978; Mbiene *et al.* 1988), and already extend their central axons into the nascent vestibular nuclei by E11.5 (Maklad *et al.* 2010). The time of first synaptic contact between vestibular primary afferents and vestibular projection neurons has yet to be determined in the mouse but it is likely that functional synaptic contacts will initially appear in the

lateral vestibular nucleus, which develops first during embryogenesis (Altman & Bayer, 1980b). Indeed, by birth neurons in the lateral vestibular nucleus are already invested with nerve endings (Karhunen, 1973) including those of the primary vestibular afferents (Morris *et al.* 1988). Finally, vestibulospinal axons in the mouse reach cervical levels by E12 (LVST) and E14 (MVST) (Auclair *et al.* 1999; Pasqualetti *et al.* 2007) and are therefore already positioned to convey the resting and afferent-evoked discharges that vestibular neurons display at birth (Lannou *et al.* 1979).

In accord with the early anatomical development of the murine vestibular system, we report here that vestibulospinal-mediated synaptic inputs to MNs are already functional in the neonatal mouse and are organized according to key tract- and segment-specific features of the adult mammalian pattern. We also provide novel information about aspects of vestibulospinal organization little or not yet explored in adults, including the pattern of overlap between MVST and LVST inputs and the presence of LVST inputs to axial MNs in the thoracolumbar cord. Preliminary reports have appeared (Kasumacic *et al.* 2008, 2010).

Methods

Brainstem–spinal cord preparation

The majority of the experiments were performed on mice of the ICR strain ($n = 80$) aged postnatal day (P) 0–5. To test the generality of our findings, experiments were also performed on an additional 13 neonatal mice of other strains that were available to us while we performed this study (BalbC, $n = 9$ and NZEG, $n = 2$, obtained from Martyn Goulding, Salk Institute; and Nkx 6.2lacZ, $n = 2$, obtained from Johan Ericson, Karolinska Institute). Mice were deeply anaesthetized with isoflurane (Abbott, Scandinavia AB). The skull was opened dorsally, and the mice were then decerebrated by transecting the brain just rostral to the superior colliculus. The mice were then placed in ice-cold glycerol-based dissecting solution (Ye *et al.* 2006; Tanaka *et al.* 2008), containing (in mM): glycerol 250, KCl 2, D-glucose 11, CaCl₂ 0.15, MgSO₄ 2, NaH₂PO₄ 1.2, Hepes 5 and NaHCO₃ 25. Within 30 min, the brainstem and spinal cord were carefully dissected out along with ventral and dorsal roots and selected cranial nerves. After dissection, the solution was immediately replaced by room temperature (24–27°C) artificial cerebrospinal fluid (aCSF) containing (in mM): NaCl 128, KCl 3, D-glucose 11, CaCl₂ 2.5, MgSO₄ 1, NaH₂PO₄ 1.2, Hepes 5 and NaHCO₃ 25.

All efforts were made to minimize the number of animals used and their suffering in accordance with the European Communities Council directive 86/609/EEC and the National Institutes of Health guidelines for the

care and use of animals. All procedures were approved by the Norwegian National Animal Research Authority (NARA).

Retrograde labelling of MNs and vestibulospinal neurons, and optical recording of calcium transients

MNs in cervical (C2 and C6), thoracic (T7) and lumbar (L2 and L5) segments were retrogradely labelled by applying crystals of Calcium Green-1-conjugated dextran amine (CGDA, 3000 MW, Molecular Probes) to the cut ventral roots using the procedure of Glover (1995). These specific segments were chosen so that we could compare the organization and developmental maturity of vestibulospinal inputs to neck, trunk and limb MNs. The cut was made very close to the root entrance to minimize labelling time. During crystal application, surplus CGDA was removed by mouth suction through a micropipette to avoid contamination of nearby roots or the spinal cord itself. Retrograde labelling was allowed to continue at room temperature in the dark for 3 h, at which time CGDA fluorescence was readily visible in the MN somata (Fig. 2A). In separate experiments ($n = 9$), we labelled vestibulospinal neurons retrogradely with either rhodamine-conjugated dextran amine (RDA, 3000 MW, Molecular Probes) or RDA combined with CGDA. In these experiments, the crystals were applied to the cut ventral and ventrolateral funiculi (VF+VLF) at the level of C1. Successful labelling of vestibulospinal neurons required an incubation time of 8–10 h at room temperature.

Preparations containing labelled MNs or vestibulo-spinal neurons were transferred to a Sylgard-coated chamber where they were pinned down ventral side up using stainless-steel (Minuten) pins. The chamber was perfused with oxygenated aCSF at a rate of 3.6 ml min^{-1} , giving a total volume exchange every 3 min. The labelled neurons were visualized through the ventral white matter with a $40\times$ water immersion objective (LUMPlanFl, 0.8 NA, Olympus, Norway) using an epi-fluorescence microscope (Axioskop FS2, Carl Zeiss, Oberkochen, Germany) equipped with a 100 W halogen lamp driven by a DC power supply (PAN35-20A, Kikusui Electronics Corporation, Japan) and excitation and emission filters (BP 450–490 nm and LP 515 nm, respectively). Fluorescence changes associated with neuronal activity, which we refer to hereafter as 'Ca²⁺ transients' or 'responses', were registered using a cooled CCD camera (Cascade 650, Photometrics, Texas Instruments, USA) mounted on a video zoom adaptor. As higher frame rates with reduced exposure times require stronger illumination and lead to rapid bleaching, image series were routinely acquired at 4 frames s^{-1} using the image-processing software Metamorph 5.0 (Universal Imaging Corporation, Molecular Devices) with the exception of the experiments described in Fig. 3. To

further minimize photo-bleaching, we used low-intensity epi-illumination and a binning factor of 2. We also limited the exposure time per recording to 2 min, during which we registered a drop in baseline fluorescence due to bleaching of only $0.36 \pm 0.35\%$ compared to $2.23 \pm 0.46\%$ after 10 min ($n = 12$ MNs examined in 3 animals).

Control experiments ($n = 4$) were performed to obtain an estimate of the extent to which light scattering in the x - y plane could contribute to responses recorded in the MNs. We found that the magnitude of the Ca²⁺ transients recorded from the somata of single MNs that were spatially isolated from other labelled MNs, fell off to about 65% ($65.5 \pm 19.3\%$) at a distance of $10 \mu\text{m}$ and to about 4% ($4.4 \pm 1.5\%$) at a distance of $100 \mu\text{m}$. Thus, substantial optical contamination of inactive MNs by nearby active MNs is limited to a few MN cell diameters.

Electrical stimulation of the VIIIth nerve

Vestibulospinal neurons were activated by stimulating the VIIIth cranial nerve with a fire-polished borosilicate glass (Harvard Apparatus, UK) suction electrode coupled to a digital stimulator (DS 8000, WPI, UK). The electrode position and suction were verified at regular intervals during the experiment. Data acquired after eventual electrode repositioning were analysed separately from previous data.

Although single pulses could elicit responses in spinal MNs, these could be recorded reliably only at relatively high frame rates which, as mentioned above, led to photo-bleaching of the CGDA. To produce responses easily detected at 4 frames s^{-1} , stimulation was delivered in the form of trains (5 s duration) of $200 \mu\text{s}$ pulses at 5 Hz, with a current strength between 60 and $500 \mu\text{A}$. Trains were delivered usually twice per 2 min recording session at an inter-train interval of 60 s to avoid synaptic fatigue. In preliminary experiments in which we tested various inter-train time intervals from 5 to 60 s (20 cells in 2 animals), we found that when two trains were separated by more than 15 s, the response in the second train was not significantly depressed compared to the response to the first train (Train₁: 22 ± 6 arbitrary units (au) vs. Train₂: 22 ± 5 au, $P = 0.87$). Stimulation strength was expressed in multiples of current threshold (T) for evoking a detectable increase in CGDA fluorescence, as defined in the Data analysis section below.

In eight animals, we tested whether current spread from the suction electrode might activate spinal circuits directly by stimulating the ventral surface of the brainstem in close proximity to the VIIIth nerve while looking for evoked responses in ipsilateral MNs ($n = 6$) or contralateral MNs ($n = 4$). The strength of the stimulation delivered at the brainstem surface was set to either $500 \mu\text{A}$ (maximal current strength used for the stimulation of

the VIIIth nerve in this study) or 1 mA. We never observed responses in either ipsi- or contralateral MNs with such high-intensity brainstem surface stimulation and therefore conclude that activation of spinal circuitry is not due to current spread through the bath.

Ventral root recording

Labelled ventral roots were recorded by positioning them at the mouth of fire-polished borosilicate glass suction electrodes filled with the same aCSF as in the recording chamber and then sucking them into an omega configuration (Fig. 3A). The recorded electrical activities were fed to a differential amplifier (DPA-2FS, NPI electronic, Germany), band-pass filtered at 30 Hz–10 kHz and digitized at 5 kHz. Waveform recording traces were analysed off-line in Clampfit 9.0 (Axon Laboratory).

Pharmacological experiments

Biccuculline (20 μ M, Tocris) and picrotoxin (PTX, 40 μ M, Sigma) were used to block GABA_A receptors, and mephensin (1 mM, Sigma) was used to reduce activity in polysynaptic pathways (Kaada, 1950; Ziskind-Conhaim, 1990; Lev-Tov & Pinco, 1992). Each was bath-applied after the brainstem or the brainstem together with the cervical spinal cord was isolated by a Vaseline barrier made at C1 or C8, respectively. The drugs were applied only to the compartment caudal to the barrier. The tightness of the barrier was verified by adding phenol red to one of the compartments.

Brainstem, cerebellum and spinal cord lesions

Brainstem, cerebellum and spinal cord lesions were performed to examine the relative contribution of the different vestibulospinal tracts and the possibility of a contribution from other descending tracts.

To restrict vestibular nerve-mediated activation to the LVST, we transected the medial longitudinal fasciculus (MLF) bilaterally from the dorsal surface at a site about 200 μ m rostral to the obex ($n = 42$). These MLF lesions extended over a distance of about 150 μ m from the midline (corresponding to the anatomical extent of the MLF in neonatal mice; Paxinos *et al.* 2007 and our own anatomical observations). To ensure that the MLF lesions had the proper breadth along the mediolateral axis, control experiments were performed. In these experiments, the ventral and ventrolateral funiculi were labelled with RDA at C1 ($n = 5$) just before making the lesions. Following 8–10 h incubation at room temperature, the labelling in the brainstem was evaluated to assess how effectively the MLF lesions eliminated retrograde labelling of either or both MVST neuron groups (Fig. 1B).

To restrict vestibular nerve-mediated activation to the LVST + iMVST or cMVST we also performed ipsilateral hemisections (at the level of the C1 segment) and contralateral hemisections (either at the level of the obex or at the level of the C1 segment; see diagrams at the top of Figs 6 and 8).

To assess the possibility of a contribution from descending pathways other than the vestibulospinal pathways, we used the results from some of the lesions described above and in addition performed either a very broad transverse lesion of the brainstem ($n = 3$, see diagram in Fig. 9Ab) or a cerebellectomy ($n = 4$).

To assess the contribution of locally crossing connections in the spinal cord (from descending vestibulospinal axons, commissural spinal interneurons and/or midline crossing dendrites from contralateral MNs), we performed a midline lesion at different levels of the spinal cord that encompassed several segments including the segment under study ($n = 9$, see rightmost diagram at top of Figs 6 and 8).

At the end of all experiments the location and actual size of the lesions was confirmed histologically. The brainstems were fixed in 4% paraformaldehyde (PFA) overnight, embedded in optimum cutting temperature formulation (OCT), frozen and sectioned at 30–100 μ m in the transverse or sagittal plane using a cryostat (Leica, CM3050S). Sections were stained with haematoxylin using a conventional procedure (5% w/v Harris haematoxylin, Sigma) and images were taken with a ProgRes C14 CCD camera mounted on an Olympus AX70 microscope, or a Hamamatsu C4880 CCD camera mounted on a Leica DMRXA microscope.

Data analysis

Circular digital apertures of identical size and shape, termed regions of interest (ROIs) in the MetaMorph software, were placed manually over individual MN somata that were clearly visible in one focal plane. Selection of MNs was done prior to stimulation and therefore was blind to the effect of the stimulation. We routinely analysed six MNs per motor column in each recording. To test whether these recordings were representative of the entire motor column, in some experiments we analysed a large number of MNs per motor column (up to 25 at a time, $n = 6$ experiments) and sometimes used much larger ROIs to analyse the entire motor column ('population response', $n = 10$). The Ca²⁺ transients in each ROI were quantified as changes in fluorescence (ΔF) divided by the baseline fluorescence F_0 before the stimulation ($\Delta F/F_0 = (F - F_0)/F_0$) to compensate for variability in the CGDA labelling intensity among MNs. The data were converted to text files using a custom-made program (Fileconvert by Bruce

Piercey) then imported into Clampfit 9.0 where they could be expressed as waveforms. A detectable response was defined as a continuous positive deflection exceeding a detection limit of two standard deviations above the mean of the baseline. Response magnitude was defined as the area under the waveform above the detection limit. The magnitudes of responses evoked in each MN during a single recording session (usually two per session) were averaged. Unless indicated otherwise, all data are presented as grand means \pm standard deviations across preparations.

Results

Optical recordings of calcium transients were obtained from individual MNs in the motor columns of segments C2, C6, T7, L2 and L5 in a total of 93 animals. In C2 and T7, somatic MNs are grouped into one medially located motor column (MMC) whereas in C6, L2 and L5 they are grouped into the MMC and a lateral motor column (LMC). In some animals recordings were made in multiple segments and on both sides. Recordings were obtained from MNs located ipsilateral ($n = 73$ animals) and/or contralateral ($n = 32$ animals) to the VIIIth nerve being stimulated. The total number of MNs in which responses were analysed exceeded 2000 and the actual number of individually visualized MNs in which responses were recorded (but not necessarily analysed) was about 2-fold higher. Unless stated otherwise, sample sizes ' n ' below refer to the number of animals from which recordings were obtained.

Synaptic activation of vestibulospinal neurons in the neonatal brainstem–spinal cord

Vestibulospinal neurons were activated indirectly by electrical stimulation of the VIIIth nerve afferents (diagram of experimental arrangement in Fig. 1A). We chose this method over direct stimulation of the vestibular nuclei because it activates vestibulospinal neurons synaptically without undesirable tissue damage due to electrode penetration and electrolysis. To test directly whether we could synaptically activate the vestibulospinal neurons, we labelled them retrogradely with CGDA and monitored their response to VIIIth nerve stimulation. We could see CGDA-labelled vestibulospinal neurons through the dorsal surface of the brainstem in the region corresponding to the vestibular nuclei. Although this protocol labels all of the three trajectory-defined groups of vestibulospinal neurons (iMVST, cMVST and LVST groups in Fig. 1Ba; Díaz & Glover, 2002; Pasqualetti *et al.* 2007), the recordings were probably dominated by neurons of the LVST group, since these are larger, more numerous and located most dorsally. The more deeply located neurons in the iMVST and cMVST groups could

not be visualized distinctly. In all experiments, nerve stimulation (single pulse or longer trains, $n = 3$) elicited simultaneous Ca^{2+} transients in all visible CGDA-labelled vestibulospinal neurons (Fig. 1C).

Although nerve stimulation may not reveal all functional connections because intervening synapses in the neonatal rodent can exhibit fatigue (for a discussion of this issue see Floeter & Lev-Tov, 1993), these experiments clearly show that vestibular nerve stimulation already leads to synaptic activation of vestibulospinal neurons by birth.

Determination of effective stimulation parameters for VIIIth nerve-evoked responses in spinal MNs and correlation of the responses with spiking activity

In the neonatal mouse, several factors may contribute to a need for stimulation parameters different from those used in adult animals. Synaptic connections from vestibular afferents may not be as mature or numerous (see, for example, Lannou *et al.* 1979), they may fatigue more rapidly, and vestibular afferent and vestibulospinal axons may not have achieved full calibre or be fully myelinated and therefore fail to propagate action potentials as reliably as in adults. Furthermore, as in adult mammals, polysynaptic connections between vestibulospinal neurons and spinal MNs may exist in addition to monosynaptic connections, and spatial and temporal summation thus may be required to activate the MNs. Therefore, to determine the most effective parameters for activating spinal MNs by VIIIth nerve stimulation, we tested a range of parameters for each of the motor columns that were found to be responsive in each of the segments investigated (Fig. 2). As reported above, a single pulse to the VIIIth nerve readily activated vestibulospinal neurons. Whereas a single pulse elicited detectable Ca^{2+} transients in spinal MNs when signals were acquired at higher frame rates (see Fig. 3), these responses were difficult to detect when the signals were acquired at 4 Hz (see Methods). Therefore, to evoke clearly detectable and stable responses at 4 Hz, we stimulated the VIIIth nerve with trains of stimuli. As shown in Fig. 2B (individual open circles), stimulating the VIIIth nerve at twice the threshold ($2T$) with a 5 s train elicited substantially larger Ca^{2+} transients than did shorter trains, and prolonging train duration to 10 s only slightly increased the response magnitude. The effect of varying stimulation frequency on the response magnitude with a $2T$, 5 s train is shown in the same graph. The average response magnitude (all motor columns and segments pooled together) more than doubled ($260 \pm 12\%$) as stimulation frequency increased from 1 to 5 Hz (Student's t test, $P = 0.013$, $n = 10$) but an increase in stimulation frequency beyond 5 Hz did not affect response magnitude significantly. This fits well with the observation that when we stimulated with 5 s trains at threshold (Fig. 2C), less

current was required only when the frequency increased from 1 to 5 Hz (Student's *t* test, $P = 0.23$, $n = 10$) but not when the frequency increased further (Student's *t* test, $P = 0.49$, $n = 12$). Finally, as reported in a previous study of reticulospinal connections in the neonatal mouse (Szokol *et al.* 2008), stimulation at 20 Hz sometimes failed to elicit responses in MNs, suggesting that response failure at this stimulation frequency may be a general feature of descending axons in the neonatal mouse. Altogether, these experiments indicate that 2T stimulation of the VIIIth

nerve with 5 s trains at 5 Hz is effective in producing clearly detectable and stable responses in spinal MNs when recording at 4 Hz. Thus, all experiments described below were performed with these specific stimulus parameters.

To examine the correspondence between vestibular-evoked Ca^{2+} responses and spiking activity in MNs, in three experiments we recorded the Ca^{2+} responses simultaneously with electrical activity in the T7 or L2 ventral roots (Fig. 3A). As shown in Fig. 3B for T7 MNs, the somatic Ca^{2+} response (average of 6 MNs)

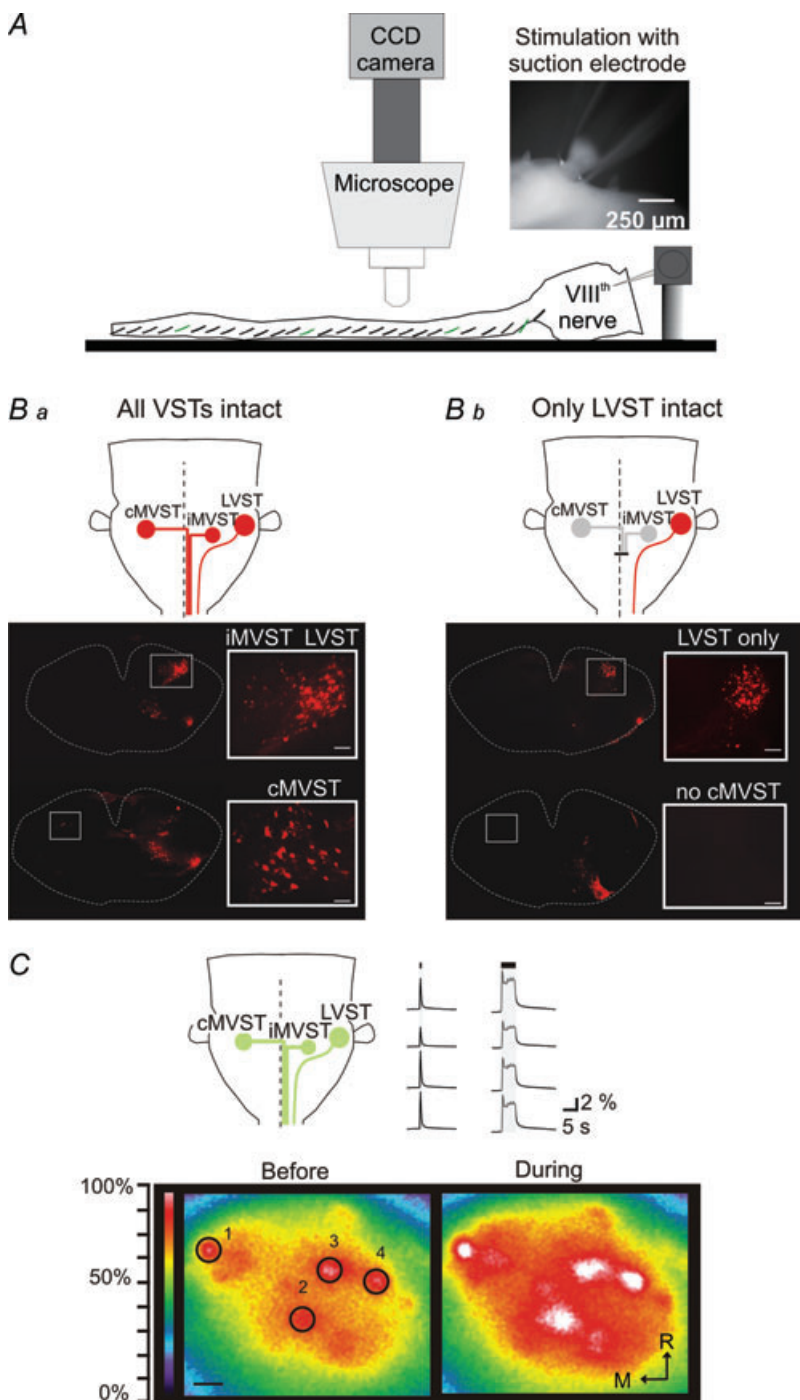


Figure 1. Brainstem–spinal cord preparation and vestibulospinal neuron activation

A, diagram of the experimental arrangement used for imaging Ca^{2+} responses in individual spinal MNs in the living brainstem–spinal cord preparation. Inset, image of a glass suction electrode placed around the proximal end of the cut VIIIth nerve for vestibular afferent stimulation. **B**, the three vestibulospinal groups investigated in this study were defined by retrograde labelling and by isolation of the LVST group by bilateral lesion of the MLF. **Ba**, rhodamine dextran amine (RDA) applied to the ipsilateral ventral and ventrolateral funiculi at C1 labels three groups of vestibulospinal neurons: two groups projecting respectively ipsilaterally and contralaterally in the MLF (iMVST and cMVST) and one group with axons projecting laterally in the medulla and spinal cord (LVST). **Bb**, RDA-labelled vestibulospinal neurons after a bilateral lesion of the MLF which interrupts the projections from both the iMVST and cMVST groups. As shown, the lesion effectively prevents retrograde labelling of the iMVST and cMVST groups, permitting the study of vestibular responses mediated by the LVST group in isolation. The scale bars on the higher magnification photomicrograph insets are 50 μm. **C**, upper left, schematic illustration of the relative locations of the 3 vestibulospinal neuron populations that give rise, respectively, to the cMVST, the iMVST and the LVST as seen after retrograde labelling and examples of responses evoked in CGDA-labelled vestibulospinal neurons during VIIIth nerve stimulation. Bottom, pseudocolour representations of the fluorescence intensities in CGDA-labelled vestibulospinal neurons (those most dorsally located and therefore principally LVST neurons) before and during VIIIth nerve stimulation (train of 5 s at 2T and 5 Hz) in a P0 mouse. An increase in Ca^{2+} fluorescence intensity during the stimulation indicates that electrical activation of the VIIIth nerve effectively activates the synaptic connections to the vestibulospinal neurons. Upper right, waveforms of fluorescence intensity in the four vestibulospinal neurons labelled 1–4. During the first session the VIIIth nerve was stimulated with a single pulse whereas during the second session the nerve was stimulated with a 5 s train. Scale bar: 50 μm.

was found to relate directly to the presence of action potentials in the axons. In this particular experiment, each train stimulus evoked a distinct Ca^{2+} transient that was associated with a burst of action potentials in the ventral root. Therefore, irrespective of whether they result from mono- or polysynaptic activation, vestibular-evoked somatic Ca^{2+} responses in MNs are good indicators of action potential activity.

Response patterns in ipsilateral MNs

In C2, stimulation of the VIIIth nerve evoked responses in the iMMC ($n = 5, 30$ MNs total). An example is shown in Fig. 4 (leftmost panel) where the fluorescence changes are shown both as a sequence of three video images before (5 s), during (15 s) and after (30 s) stimulation, and as a waveform. Typically, the responses had a sharply rising

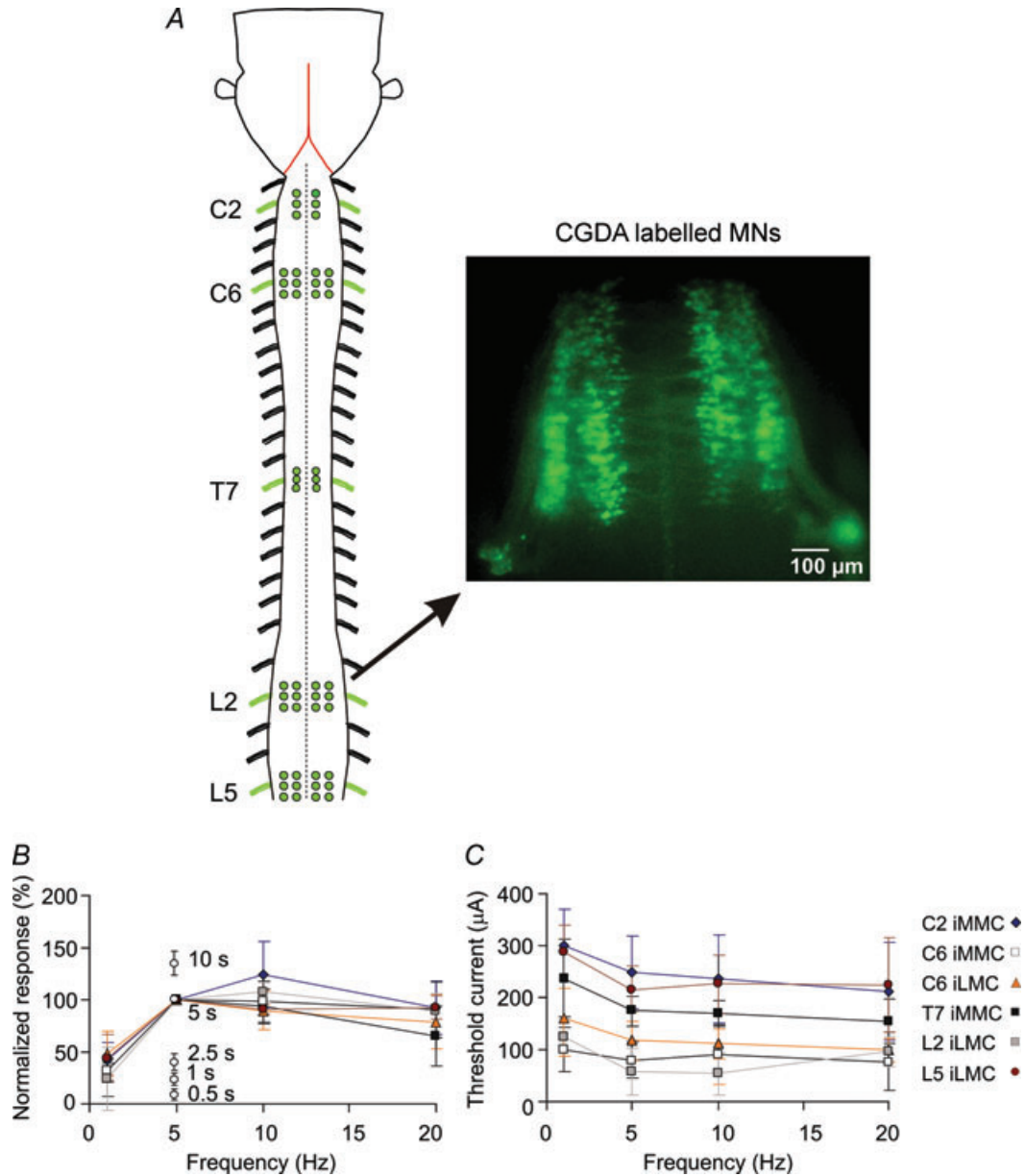


Figure 2. Motoneuron labelling for optical recording and effective stimulation parameters
 A, schematic overview of labelled MNs in different segments (left) and photograph of CGDA-labelled MNs in L2 (right). B and C, effective stimulation parameters for evoking Ca^{2+} responses in iMMC or iLMC in the different spinal segments investigated. The graph in B displays the amplitude–frequency curves when stimulating at 27 with a 5 s train and the response magnitudes as a function of train duration when stimulating at 27 and 5 Hz (individual open circles). Each response is an average (total of 4 experiments or 20–76 MNs) and is expressed as a percentage of the response at 5 Hz. The graph in C displays the magnitudes of the responses elicited by stimulating the VIIIth nerve at threshold current (T) with a 5 s train, as a function of frequency. Each response is an average of 4 experiments (5–19 MNs per experiment). All values are means \pm standard deviations.

initial peak followed by a lower-magnitude plateau during the stimulus train on which smaller peaks often occurred and, in some cases, also a tail that continued after the end of the stimulus train.

In C6, VIIIth nerve stimulation evoked responses in both the iMMC and the iLMC ($n = 13$, 162 MNs total). The responses in the iMMC and iLMC began with a

sharp initial peak followed by a lower-magnitude plateau that often rose during the stimulus train and sometimes (most often in the iMMC) exhibited another sharp peak at the end of the stimulus train that could approach and even surpass the amplitude of the initial peak (Fig. 4, second panel). The responses also typically had a tail that continued after the end of the stimulus. The response

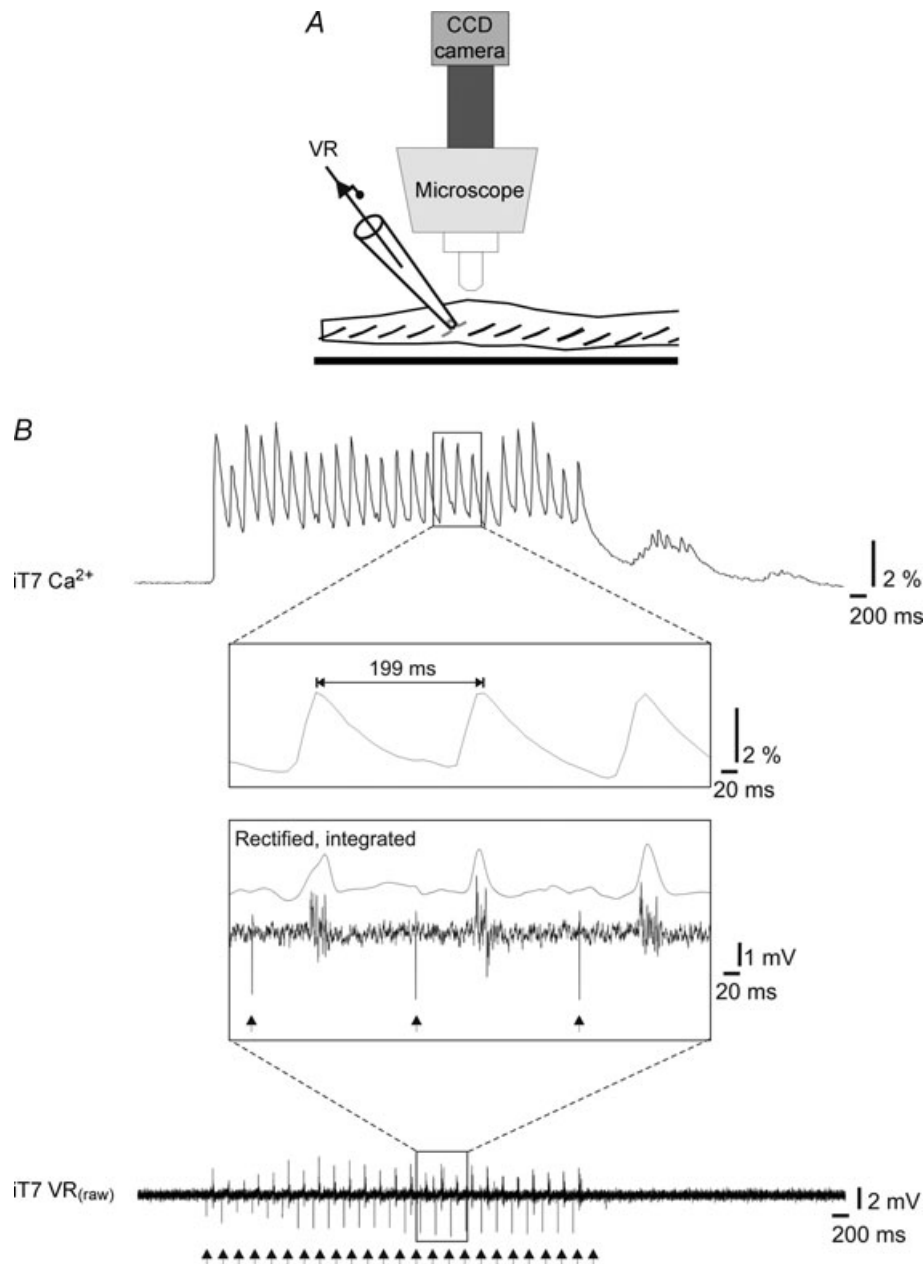


Figure 3. Correspondence between somatic Ca^{2+} responses and ventral root discharge

A, after retrogradely labelling the T7 ventral root (VR) with CGDA-1, the root was inserted in a suction electrode to record the axonal discharge. *B*, simultaneous recordings of the calcium response from T7 MNs (top) and the MN population discharge in the T7 ventral root (bottom) during electrical stimulation of the VIIIth nerve. The Ca^{2+} signal here was recorded at 100 (rather than the usual 4) frames per second and the ventral root signal was recorded at 5 kHz. As best shown in the insets between the traces, each Ca^{2+} transient corresponded to a burst of activity in the ventral root. In the lower inset, the rectified and integrated ventral root signal was added to facilitate comparison. Vertical arrows at the bottom indicate stimulation artefacts on the ventral root recording.

magnitudes (areas under the curve) in the MMC were similar to those in the LMC, with normalized MMC/LMC ratios of 0.91 ± 0.29 .

In T7, VIIIth nerve stimulation elicited responses in the iMMC ($n = 5$, 30 MNs total). As in C2 and C6, the responses began with a sharp initial peak. However, in contrast to C2 and C6, this sharp peak was followed by a plateau that was larger in amplitude than the initial peak and which dropped sharply at the end of the stimulus train (Fig. 4, third panel), to continue as a post-stimulus tail during which a second burst of smaller peaks was often seen. The responses in T7 were typically of larger overall magnitude than the responses in cervical or lumbar segments.

In L2 ($n = 36$, 378 MNs total) and L5 ($n = 5$, 60 MNs total) vestibular-evoked responses were not detected in the iMMC but were clearly present in the iLMC (Fig. 4, two rightmost panels). In L2, the lack of detectable response in the iMMC appeared to be a genuine absence since there was still no response after blockade of GABA_A receptors with bicuculline (described in more detail below). In the iLMC, the response was typically of small

magnitude during the stimulus train followed by a larger component that appeared only after the end of the stimulus train (Fig. 4, second to last panel). In control experiments in which the stimulus train was prolonged from 5 s to 10 or 20 s ($n = 3$), the larger component still started only after the end of the stimulus train indicating that it is a post-stimulation event. In L5, the iLMC response most often resembled the C6 iLMC response (Fig. 4, rightmost panel). Sometimes, however, the response had a shape similar to that seen in the iLMC of L2, beginning with a lower-magnitude component but with the larger-magnitude component starting during or towards the end of the stimulus train rather than immediately after (Fig. 6, bottom of third column).

To test whether the responses evoked in the ipsilateral MNs (measurements made on six MNs per motor column) were representative of the entire motor column, in some experiments we analysed a large number of MNs per motor column (up to 25 MNs, $n = 6$) or used a much larger ROI to analyse the population response from the entire motor column ($n = 10$). In both cases we observed the exact same response patterns as described above.

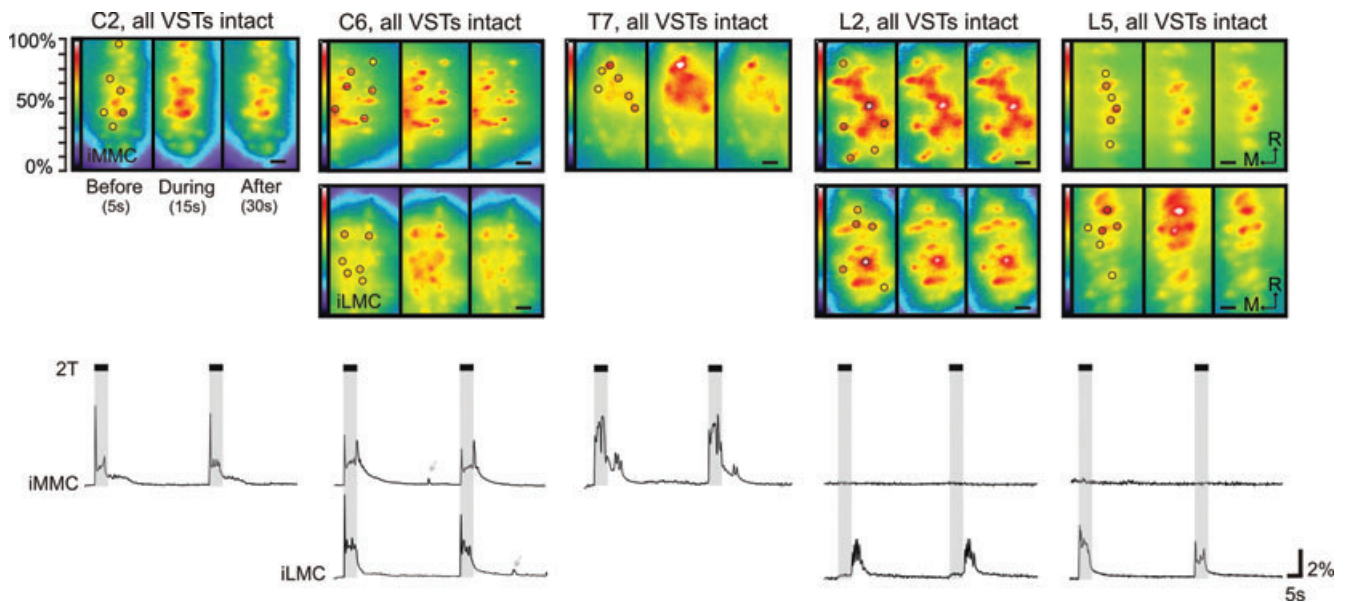


Figure 4. Vestibular-mediated response patterns in ipsilateral MNs of the cervical, thoracic and lumbar segments

Sequential recordings of the fluorescence activity in CGDA-labelled MNs in iMMC alone (C2 and T7 segments) and both iMMC and iLMC (C6, L2 and L5 segments) before, during and after VIIIth nerve stimulation at 5 s, 5 Hz, 27. The postnatal ages at which the recordings shown were made are: P1 (C2), P1 (C6), P3 (T7), P4 (L2) and P2 (L5). Each set of data comprises a series of three high magnification micrographs shown as pseudocolour representations (250 ms frame duration) of the fluorescence intensity at 5, 15 and 30 s from the onset of the recording session (i.e. before, during and after the stimulation) and corresponding average waveforms ($n = 6$ MNs or ROIs) showing the changes in fluorescence throughout the entire 120 s recording session. The pseudocolour representations were made by filtering the complete image series of the recording session in Metamorph with a low pass 3×3 filter and then converting greyscale values to colours using a rainbow index, with transition from blue to red to white representing increasing response size. On the first of each series of three frames, the circles indicate the location of the manually defined ROIs placed over 6 MNs in each motor column, and on the last frame, the scale bar is $50 \mu\text{m}$. The duration of the stimulation is shown on the waveform displays with vertical grey shading. Grey arrows indicate occasional spontaneous increases in Ca^{2+} fluorescent.

Effects of mephenesin and GABA_A receptor antagonists on ipsilateral responses

Mephenesin has been shown to reduce transmission in descending polysynaptic pathways in neonatal brainstem–spinal cord preparations of the rat (Floeter & Lev-Tov, 1993; Vinay *et al.* 1995; Juvin & Morin, 2005). To test whether polysynaptic pathways contributed to the responses evoked by vestibular nerve stimulation, we examined the effects of mephenesin (1 mM) application on the evoked responses in the MNs of C2, T7 and L2 segments in six animals. As shown in Fig. 5A, mephenesin reduced the Ca²⁺ responses in all three segments by more than 50% with the largest reductions seen in the MMC MNs of T7 (reduced to $5.70 \pm 0.3\%$ of control response, $n = 18$ MNs, Fig. 5B).

As a preliminary investigation of the nature of the synaptically mediated Ca²⁺ responses in ipsilateral MNs, in seven animals we also examined the effects of the GABAergic antagonists bicuculline (20 μ M) and PTX

(40 μ M) on the responses in C2 and L2 (Fig. 5C). In C2, blockade of GABA_A receptors with bicuculline did not affect much the initial, sharply rising peak of the iMMC response but increased the magnitude and duration of the following plateau. The duration of the plateau was prolonged beyond the end of the stimulus train, more than tripling the total magnitude (area under the curve) of the responses (Fig. 5D). Since bicuculline has non-specific direct effects on neonatal MNs (see Pflieger *et al.* 2002 in the neonatal rat), we also examined the effects of PTX. Similar to bicuculline, PTX increased the vestibular-mediated responses in C2 MNs (Fig. 5C). The increase in response following PTX application was larger than following bicuculline application, reaching up to 800% of control response (Fig. 5D).

In L2, the presence of bicuculline or PTX ($n = 4$, not shown) did not reveal any covert responses in the iMMC. However, both blockers changed the response pattern in the iLMC. As shown in Fig. 5C (second row), bicuculline increased the magnitude of both the first component

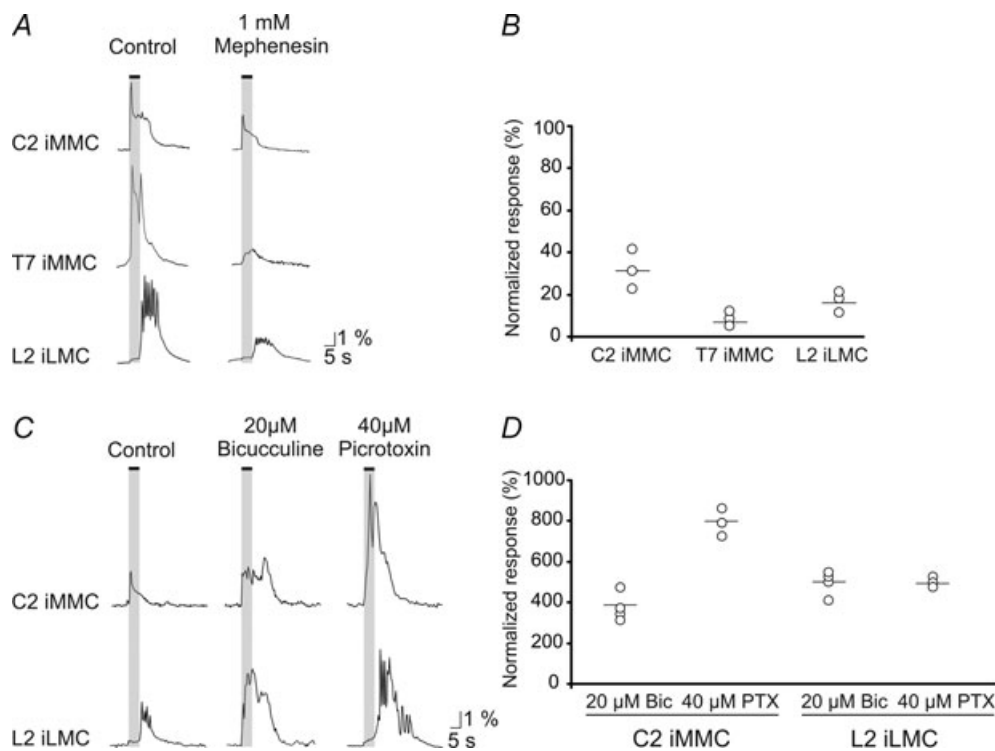


Figure 5. Mephenesin strongly reduces the magnitude of the vestibular-mediated responses and blockade of GABA_A receptors reveals an inhibitory component in the iMMC response of C2 and the iLMC response of L2

A, responses evoked during electrical stimulation of the VIII nerve with a 5 s train at 5 Hz (2T) in the iMMC of C2 and T7 and the iLMC of L2 before (traces on the left) and after (traces on the right) application of mephenesin to a split-bath compartment containing the cervico-thoraco-lumbar or thoraco-lumbar regions of the spinal cord. B, graph showing the magnitudes of the responses during mephenesin application, normalized to the control response. Each point shows the average response in a single preparation and the horizontal lines indicate the grand mean. C, left traces, responses evoked during electrical stimulation of the VIII nerve with a 5 s train at 5 Hz (2T) in the iMMC of C2 and the iLMC of L2. Middle and right traces, effects of 20 μ M bicuculline and 40 μ M PTX on these responses. D, graph showing the magnitudes of the responses during application of each drug, normalized to the control response. Each point shows the average response in a single preparation and the horizontal lines indicate the grand mean.

and the post-stimulation component. Application of PTX produced a similar increase in the magnitude of the response in the iLMC of L2 but in contrast to bicuculline the first component seemed hardly affected (Fig. 5C and D).

Together these results indicate that responses in ipsilateral MNs are mediated at least in part by polysynaptic pathways involving mixed excitatory and inhibitory inputs (see Discussion).

Relative contributions from the MVSTs and the LVST to ipsilateral responses

To investigate the relative contributions of the three vestibulospinal tracts (LVST, iMVST and cMVST) to responses in ipsilateral MNs, we compared in the same preparation the responses to stimulation of the VIIIth nerve before and after various lesions (see diagrams in Fig. 6) including: (1) ipsilateral hemisection at C1 ($n = 6$),

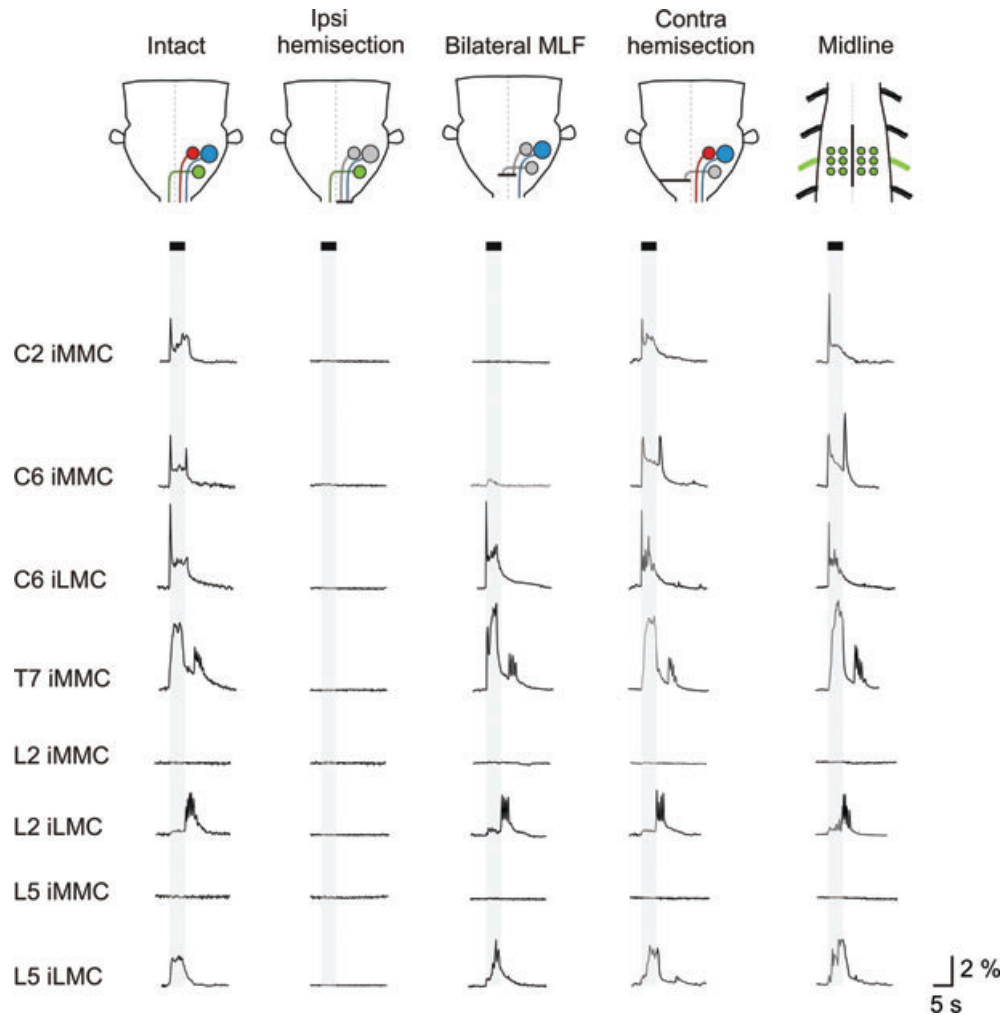


Figure 6. Effects of various lesions on vestibular-mediated response patterns in ipsilateral MNs

From top to bottom, traces showing the averaged response ($n = 6$ MNs) evoked in ipsilateral MNs in each of the segments studied. Each trace represents data from an individual experiment. The first and third columns show the typical responses in intact preparations and preparations with a bilateral MLF lesion, respectively (C2 and C6 from P2 mice, T7 from a P1 and a P4 mouse, L2 from a P3 and a P2 mouse and L5 from P3 mice). The second column (ipsilateral hemisection) and the last two columns (contralateral hemisection and midline spinal cord lesion) are from different experiments (ipsilateral hemisection: C2, C6, T7, L2 and L5 from P2 mice, contralateral hemisection: C2 from a P2 mouse, C6 from a P3 mouse, T7 and L2 from P1 mice and L2 from a P2 mouse, midline lesion: C2, C6, T7, L2 and L5 from P3 mice). The contralateral hemisections were performed either at the level of the obex (C2 and C6) or at C1 (T7, L2 and L5).

which interrupts transmission via the iMVST and LVST and all other ipsilaterally descending brainstem pathways that may have been activated by the stimulation, (2) bilateral lesion of the MLF ($n=17$), which interrupts transmission via the iMVST and cMVST as well as all other MLF-projecting descending pathways, (3) contralateral hemisection either at the level of the obex or the C1 segment ($n=9$), which interrupts transmission via the cMVST and all other contralateral brainstem descending pathways and (4) midline lesion ($n=3$) to investigate the possibility of a contribution from crossing vestibulospinal axon collaterals, local excitatory commissural spinal interneurons or midline-crossing MN dendrites. However, as expected, the latter lesion had no obvious effect on ipsilateral responses in the segments examined.

In C2 (top row in Fig. 6), ipsilateral hemisection ($n=3$, second column in Fig. 6) and bilateral MLF lesion ($n=5$, third column in Fig. 6 and graph in Fig. 7) abolished responses in the iMMC whereas contralateral hemisection had no obvious effect ($n=3$, fourth column in Fig. 6). This indicates that the iMMC responses in C2 are mostly, if not entirely, mediated by the iMVST.

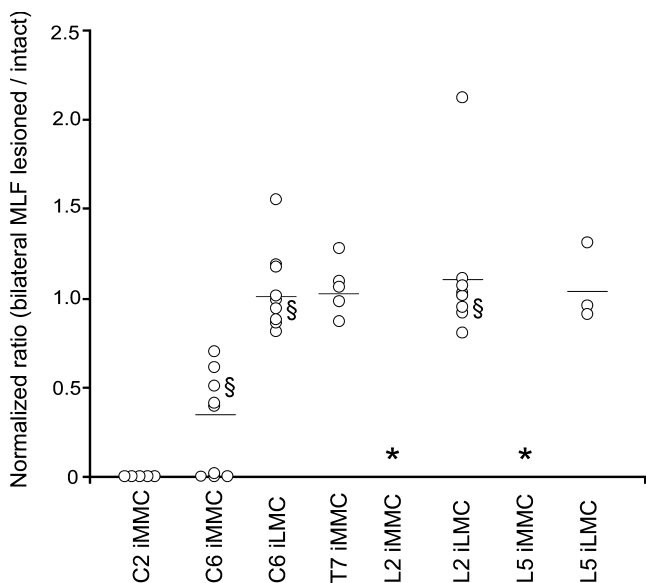


Figure 7. Graphical summary of the effects of bilateral MLF lesion on the response patterns in ipsilateral MNs

The graph displays the normalized response ratios in ipsilateral MNs, obtained by directly comparing the responses before and after bilateral MLF lesion in the same preparation. Each data point represents a single preparation and the horizontal lines indicate the grand mean ratio. The bilateral MLF lesion eliminated the response in the iMMC of C2 and greatly decrease the iMMC responses in C6 but had no significant effect on the iMMC responses in T7. In L2 and L5, VIIIth nerve stimulation remained ineffective in evoking responses in the iMMC (indicate with an asterisk) and had no significant effect on the LMC responses. § indicates that the data point is from an experiment performed in a mouse strain other than ICR (Balb C, N-ZEG or Nkx 6.2lacZ).

In C6 (second and third row in Fig. 6), ipsilateral hemisection abolished the responses in both iMMC and iLMC ($n=3$), whereas bilateral MLF lesion significantly decreased the iMMC response without affecting the iLMC response ($n=9$, Mann–Whitney, $P=0.002$, $U=36$ for iMMC and $P=0.597$, $U=73.5$ for iLMC), and contralateral hemisection had no obvious effect ($n=3$). The average ratios of the post-MLF lesion responses to responses in intact preparations were $0.29 \pm 0.3\%$ and $1.04 \pm 0.2\%$, respectively (Fig. 7). This indicates that the iMMC responses in C6 are mediated by both the iMVST and the LVST whereas the iLMC responses are mediated mostly, if not entirely, by the LVST alone.

In the thoracic and the lumbar segments (five bottom rows in Fig. 6), ipsilateral hemisection abolished the responses in the iMMC (T7, $n=2$) and iLMC (L2 and L5, $n=2$) whereas neither bilateral MLF lesion (Mann–Whitney, $P=0.524$, $U=31$ and $n=5$ for T7; $P=0.590$, $U=92$ and $n=9$ for L2 and $P=0.671$, $U=30$ and $n=5$ for L5) nor contralateral hemisection (T7, L2 and L5, $n=3$) had any obvious effect. The average ratios of the post-MLF lesion responses to the responses in intact preparations were 0.98 ± 0.13 in T7, 1.04 ± 0.33 in L2 and 0.95 ± 0.29 in L5 (Fig. 7). This indicates that responses in thoracic and lumbar segments are mediated by the LVST alone.

Response patterns in contralateral MNs

Examples of responses evoked in contralateral MNs in intact preparations are displayed in Fig. 8 (first column). In C2 ($n=5$, 40 MNs) and C6 ($n=8$, 64 MNs), the magnitudes and the patterns of the responses in contralateral MNs differed somewhat from their ipsilateral counterparts. For instance in C6, the response magnitudes in the cMMC were somewhat larger than those in the cLMC, with a cMMC/cLMC ratio of 1.35 ± 0.65 (Mann–Whitney, $P=0.046$, $U=48.5$ and $n=8$). With regards to the response patterns, the responses in the cMMC of C2 and C6 typically (but not always) lacked the initial peak seen in the ipsilateral responses (compare the response in Fig. 6 to the response in Fig. 8).

In T7 ($n=5$, 48 MNs), the responses in contralateral MNs were very similar to those recorded in ipsilateral MNs (Mann–Whitney, $P=0.197$, $U=36$). One exception, however, was the second burst of activity after the end of the stimulus that was often seen in the iMMC but was rarely observed in the cMMC (compare Figs 6 and 8).

In L2 and L5 ($n=16$ for a total of 192 MNs in L2, and $n=5$ for a total of 60 MNs in L5), the responses evoked in the contralateral MNs differed in many respects from the responses evoked in the ipsilateral MNs. First, in contrast to the ipsilateral side where we detected responses only in the LMC, responses were detected in

both the cLMC and the cMMC (see Fig. 8 for a direct comparison of the responses in cLMC and cMMC and the Supplementary Video for comparison of iMMC and cMMC), with cMMC/cLMC response ratios of 0.55 ± 0.34 in L2 and 0.42 ± 0.21 in L5. Second, in contrast to the responses evoked in the iLMC of L2 (and sometimes also in L5) where the largest response occurred after the stimulation train ended, in all experiments the responses evoked in the cLMC were largest during the stimulus train with a sharp rise at stimulus onset and a rapid decline from stimulus termination (compare Figs 6 and 8). Third,

the responses in the cLMC (but not the iLMC) of L5 sometimes displayed a second, smaller burst of activity after the end of the stimulation (Fig. 8).

Relative contributions from the MVSTs and the LVST to contralateral responses

To investigate the contributions of the three vestibulospinal tracts to responses in contralateral MNs, we compared the responses to stimulation of the VIIIth nerve before and after the same lesions used

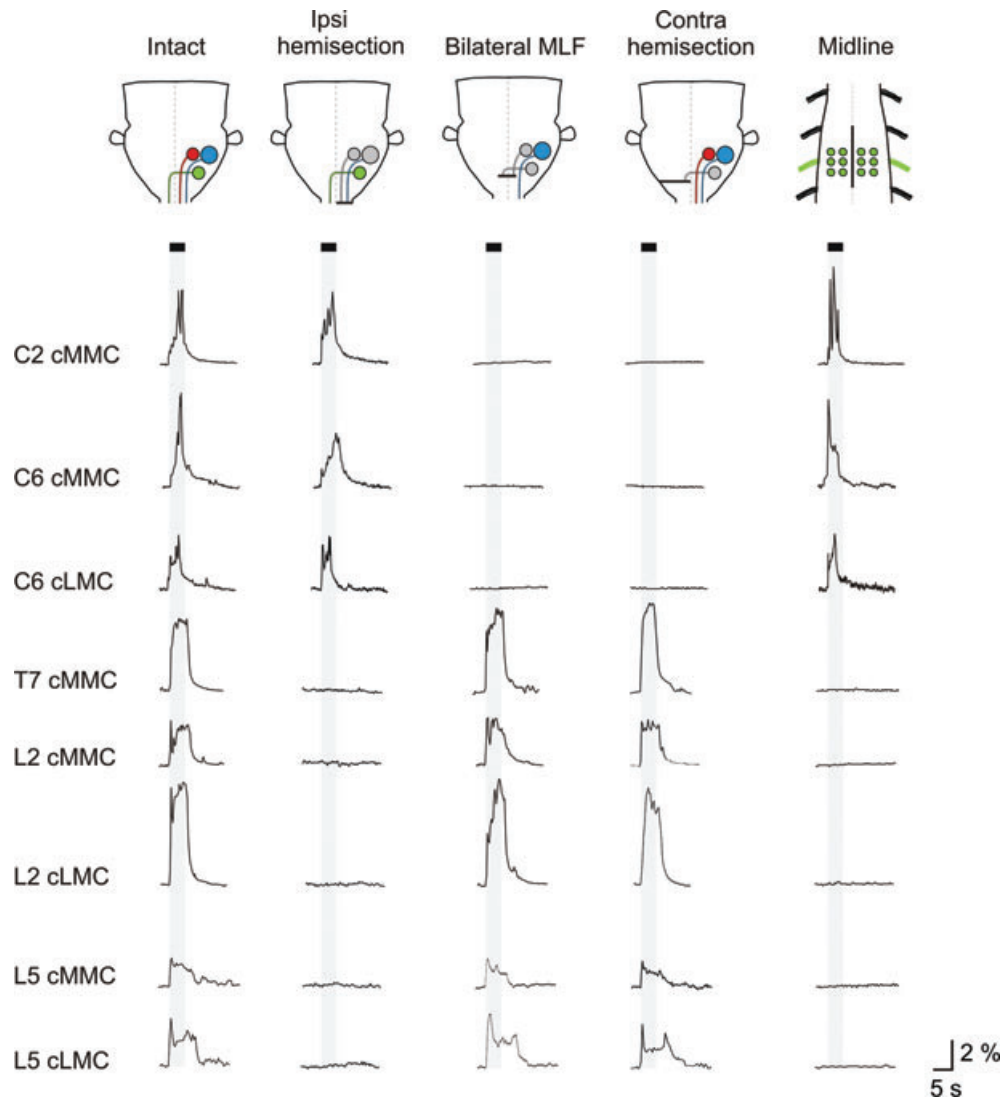


Figure 8. Vestibular-mediated response patterns in contralateral MNs and effects of various lesions

From top to bottom, traces showing the averaged response ($n = 6$ MNs) evoked in contralateral MNs in each of the segments studied. Each trace represents data from an individual experiment. The data shown in the first and the third columns (intact and bilateral MLF lesion) are from the same experiments (C2 and C6 from a P1 mouse, T7 from a P2 mouse, L2 from a P3 mouse and L5 from a P2 mouse). The second column (ipsilateral hemisection) and the last two (contralateral hemisection and midline spinal cord lesion) are from different experiments (ipsilateral hemisection: C2 and C6 from P2 mice, T7 from a P3 mouse, L2 and L5 from P1 mice; contralateral hemisection: C2 and C6 from P1 mice, T7 and L2 from P3 mice and L5 from a P2 mouse; midline lesion: C2 and C6 from P2 mice, T7 and L2 from P3 mice and L5 from a P2 mouse). The contralateral hemisections were performed either at the level of the obex (C2 and C6) or at C1 (T7, L2 and L5).

in assessing ipsilateral responses, namely ipsilateral hemisection at C1 ($n=3$), bilateral lesion of the MLF ($n=12$), contralateral hemisection at the level of the obex or at C1 ($n=11$) and midline lesions ($n=9$) (see diagrams in Fig. 8).

In C2 and C6, ipsilateral hemisection had no effect on any of the contralateral responses ($n=3$). In contrast, bilateral MLF lesion (third column in Fig. 8, $n=5$ in C2, $n=9$ in C6) and contralateral hemisection (fourth column in Fig. 8, $n=8$ for both C2 and C6) each completely abolished the contralateral responses. Since as mentioned above contralateral hemisection had no obvious effect on any of the ipsilateral responses, these data indicate that the contralateral responses in C2 and C6 are mediated primarily by the cMVST. Midline lesions encompassing three segments (C1–C3 or C5–C7) did not significantly affect the magnitudes of the responses in the cMMC of C2 (Mann–Whitney, $P=0.834$, $U=29$, $n=4$) or the cMMC or LMC of C6 ($P=0.832$ and 0.676 , $U=26$ and 24 , $n=4$ in both cases), but did result in the appearance of sharp rising peaks at the onset of the stimulation that were not present before midline lesion (compare first and last column in Fig. 8). Although this supports the notion that all contralateral responses in cervical segments are mediated primarily by the cMVST with little contribution from locally crossing excitatory connections, it also suggests a contribution from locally crossing inhibitory connections that mask an initial sharply rising component in the cMVST-evoked response.

In the thoracic and lumbar segments, the contralateral responses were completely eliminated by ipsilateral hemisections ($n=3$ for T7, L2 and L5) whereas bilateral lesions of the MLF ($n=3$ in T7, $n=6$ in L2 and $n=3$ in L5) and contralateral hemisections at C1 ($n=3$ for T7, L2 and L5) had no obvious effect on the magnitudes of these responses (Fig. 8, Mann–Whitney, $P=0.200$, $U=47.7$ for L2). This indicates that contralateral responses in both thoracic and lumbar segments are mediated solely by the ipsilateral LVST. Midline lesions encompassing T6 to T8 ($n=3$) or L1 to L6 ($n=6$) eliminated all responses in the cMMC in T7 and the cMMC and cLMC in L2 and L5, respectively (Fig. 8, last column). Therefore, in contrast to cervical segments, locally crossing excitatory connections contribute significantly to all the contralateral responses in thoracic and lumbar segments. Whether this involves crossing LVST axon collaterals, excitatory commissural interneurons or crossing MN dendrites remains to be seen.

Effect of brainstem and cerebellum lesions

Many descending neurons other than vestibulospinal neurons have been found to be synaptically activated, although indirectly, by vestibular afferents in adult

mammals (see Peterson, 2004 for review). Two of these descending neuron populations, the reticulospinal and interstitiospinal neurons, have well-developed projections to the spinal cord in the newborn rodent (Lakke, 1997) whereas cerebellospinal and trigeminospinal projections are less developed (Leong *et al.* 1984). The possibility thus arises that some of these descending pathways might contribute to the responses reported here. To address the issue further, we tested the effects of a cerebellectomy ($n=4$) and of a broad transverse lesion of the brainstem ($n=3$) on the ipsilateral responses evoked in C6, T7 and L2 (see Fig. 9).

Removal of the cerebellum did not affect the patterns of the responses in any of the segments assessed (C6, T7 and L2, all recorded in three preparations) and the magnitudes of the responses before and after cerebellectomy were similar (cerebellectomized/intact ratio of 1.01 ± 0.23 , not shown). Hence, the possibility of a major contribution from vestibular activation of cerebellospinal neurons is unlikely.

Extensive transverse lesions of the brainstem that were broad enough to interrupt all descending and ascending fibres on the contralateral side, plus the iMVST, all ipsilateral pontine reticulospinal pathways, some ipsilateral medial medullary reticulospinal pathways and some of the LVST (compare schematics in Fig. 9*Aa* and *b*) greatly reduced but did not abolish completely the ipsilateral responses in C6 and T7, and left ipsilateral responses in L2 unaffected ($n=3$).

More specifically, in C6 the transverse brainstem lesion reduced the responses to $31 \pm 8\%$ of the control response in the iMMC and $50 \pm 1\%$ in the iLMC (graph in Fig. 9*B*). The decrease in the iMMC was similar to that observed upon bilateral MLF lesion (reported above, see Fig. 7) and therefore can be fully explained by the interruption of the MVSTs (and any other descending axons coursing in the MLF). The decrease in the iLMC on the other hand was larger than that observed upon bilateral MLF lesion, suggesting it is probably attributable to the transection of some LVST axons by the lesion (shown in blue in Fig. 9*Ab*). However, for neither the iMMC nor the iLMC responses can we exclude entirely the possibility of contributions from other ipsilateral descending axon populations that also remained intact after the brainstem lesions. In T7, brainstem lesions reduced the responses in the iMMC to $57 \pm 18\%$ (Fig. 9*B*). Such reduction in response was, however, not seen after bilateral MLF lesion (Fig. 7). Finally, in L2, brainstem lesions did not affect the responses in the iLMC (Fig. 9*B*). Therefore, the remaining 40% of the responses in the iMMC of T7 and the entire response in the iLMC of L2 might all be attributable to the contingent of LVST axons that remained intact after the lesion. Once more, however, we cannot exclude entirely the possibility of contributions from other descending axon populations that remained after

the brainstem lesion. In particular, descending projections from laterally located medullary reticulospinal neurons and trigeminospinal neurons (black dots in Fig. 9*Ab*; see also Szokol *et al.* 2008) were still intact after the lesion. To date, no vestibulo-reticulospinal projection involving laterally located medullary reticulospinal neurons has been reported in the rodent, but a vestibulo-trigeminal projection has been described anatomically (Buisseret-Delmas *et al.* 1999). Direct stimulation of the trigeminal nerve and of the region containing the laterally located reticulospinal neurons in the same brainstem–spinal cord preparation used here has been shown to elicit a substantial response in the iMMC of L2 (Szokol *et al.* 2008). This is in striking contrast to the absence of iMMC responses to VIIIth nerve stimulation, which suggests to us that trigeminospinal and lateral reticulospinal axons are unlikely to be strongly activated by vestibular nerve stimulation in the neonatal mouse.

To summarize, results from these lesion experiments are consistent with the interpretation that responses

elicited by VIIIth nerve stimulation are mediated primarily by vestibulospinal neurons, although some non-vestibulospinal contribution may be present in cervical and thoracic segments. The lesion results also underscore the primacy of LVST axons in mediating lumbar MN responses. A summary diagram in Fig. 10 shows the specific contributions of the different populations of vestibulospinal neurons deduced from our experiments.

Discussion

Using a high throughput optical approach to detect functional synaptic connections (Szokol *et al.* 2008; Szokol & Perreault, 2009), we show that vestibulospinal inputs to MNs are already established in the newborn mouse. The segmental pattern of connections was assessed comprehensively by analysing recordings at single cell resolution of over 2000 MNs as well as population

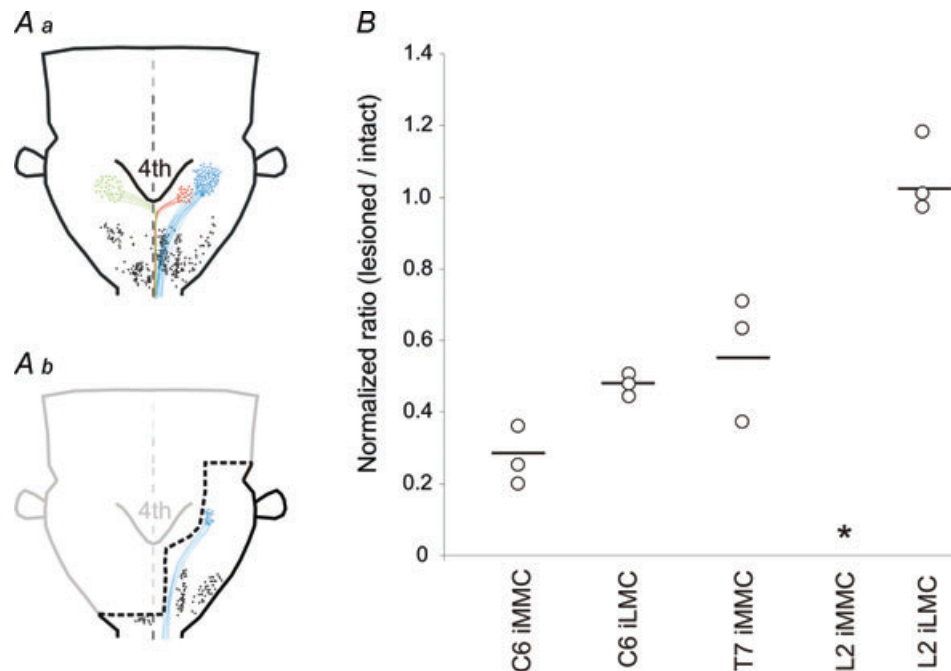


Figure 9. Effects of lesions that sever most reticulospinal projections on vestibular nerve-evoked responses in spinal MNs

Aa and *Ab*, diagrams showing the distribution of retrogradely labelled neurons following application of RDA to ipsilateral VF + VLF at the level of C1. The distribution in *Aa* was plotted from an intact preparation (P2 mouse) and that in *Ab* from a preparation in which a broad transverse lesion of the brainstem was made (thick dashed black line, P2 mouse). iMVST, cMVST and LVST neurons are shown together with their axonal trajectories in red, green and blue, respectively, and reticulospinal and trigeminospinal neurons are shown as black dots. For the sake of clarity, each dot represents 1–3 retrogradely labelled neurons in the case of vestibulospinal neurons and 4–6 retrogradely labelled neurons in the case of the reticulospinal and trigeminospinal neurons. As shown, such a large brainstem lesion interrupted many descending connections including all contralateral projections, all iMVST projections, all medial reticulospinal projections and more than 50% of the LVST projections. Some of the ipsilateral projections including part of the LVST projection and all lateral reticulospinal and trigeminospinal projections were left intact. *B*, graph showing the normalized response ratios obtained by directly comparing the responses before and after the brainstem lesion in the same preparation. Each data point is from a single preparation and the horizontal lines indicate the grand mean.

recordings of MN columns in cervical, thoracic and lumbar segments, allowing us to propose an overall functional organization of vestibulospinal inputs to axial and limb MNs (Fig. 10). As described in more detail below, connections to neck, fore- and hindlimb MNs display a pattern similar to that previously described in adult mammals. We have extended this description by discriminating inputs from the distinct iMVST and cMVST neuron populations (Glover & Petursdottir, 1988; Glover, 2000a; Pasqualetti *et al.* 2007) and by describing novel connections to axial MNs hitherto uncharacterized in mammals. The proposed organization

provides a comprehensive platform for further functional characterization of vestibulospinal inputs and a better comparative understanding of vestibulospinal projections in the vertebrate radiation (Van Mier & ten Donkelaar, 1984; Glover & Petursdottir, 1988; Pflieger & Cabana, 1996; Bussi eres *et al.* 1999; Glover, 2000a; D iaz *et al.* 2003; Zelenin *et al.* 2003; McCluskey *et al.* 2008).

Technical considerations

Due to technical limitations, we stimulated the entire VIIIth nerve without separating the vestibular component from the auditory component and, more importantly, without selectively stimulating afferents from the five individual vestibular end-organs. Although attempts were made to separately stimulate distal branches of the nerve, their investment within the labyrinth and their small size in the neonate, made the surgery simply too tedious. Although these difficulties may be more easily overcome in older animals, the extra time required to complete the dissection compromises the health of the *ex vivo* preparation and thus of functional assessment of synaptic connections. In the adult mouse, selective activation of otolith and semicircular canal afferents both generate responses in spinal MNs (Takemura & King, 2005; Sheykhosslami *et al.* 2009) and it is therefore likely that the vestibular-mediated responses we have recorded in this study were due to the activation of some or all of these afferents. Still, the pattern of connections mediated by the individual vestibular end-organs in the neonate remains to be characterized.

Other technical issues that affect the interpretation of the recorded responses, particularly with respect to the monosynaptic or polysynaptic nature of the responses, include the limited temporal resolution of the optical recordings (250 ms frame duration) and the possible spread of Ca^{2+} through gap junctions. The latter issue has been discussed previously (Szokol *et al.* 2008; Szokol & Perreault, 2009) and will not be dealt with here. However, with regards to the synaptic nature of the vestibular-mediated responses, the fact that mephenesin application significantly reduced the vestibular-mediated Ca^{2+} responses without abolishing them supports the view that these responses are mediated through both mono- and polysynaptic vestibulospinal pathways.

Two final issues concerning the nature of the evoked Ca^{2+} signals were also addressed in the present study and warrant discussion. First, we show that vestibular nerve-evoked Ca^{2+} transients in spinal MNs of the neonatal mouse brainstem–spinal cord preparation are at least partly explained by the generation of postsynaptic action potentials (Fig. 3). A similar correspondence between Ca^{2+} responses and MN firing has been reported previously in the isolated neonatal rodent spinal cord

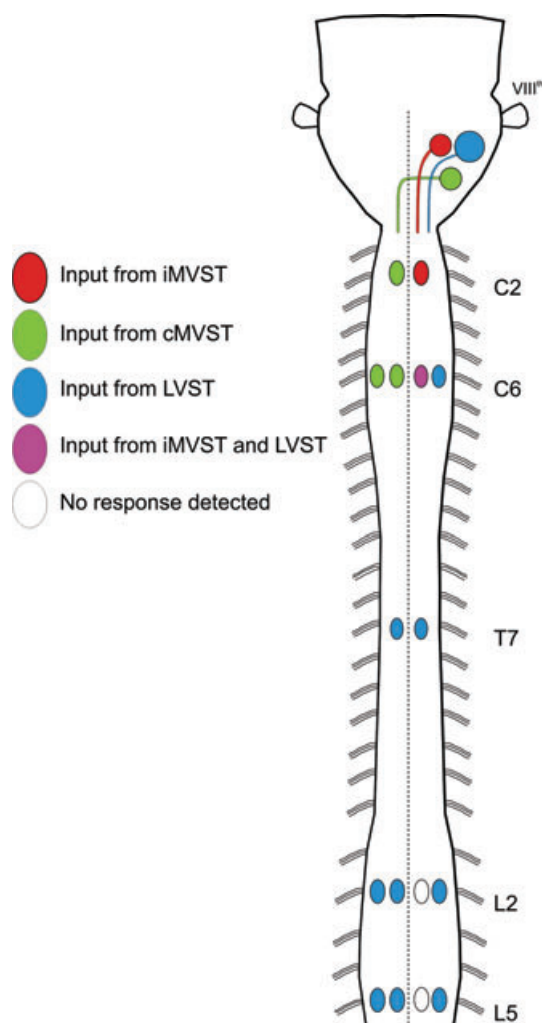


Figure 10. Proposed functional organization of vestibulospinal inputs to axial and limb MNs in the neonatal mouse

Schematic representation of a neonatal mouse brainstem and spinal cord summarizing the vestibulospinal synaptic connections to ipsi- and contralateral axial and limb MNs observed in this study. A colour code (shown on the left) is used to show the pattern of connections from each vestibulospinal group to the various groups of MNs in the different spinal segments. The connections represent both mono- and polysynaptic connections and include both excitatory and inhibitory components.

(O'Donovan *et al.* 1993; Lev-Tov & O'Donovan, 1995). Second, we demonstrate that bicuculline and PTX both increase the magnitudes of the Ca^{2+} responses in MNs. Although it is difficult to predict the effect of network activity on the different types of spinal neurons without directly recording their intracellular electrical activity, based on the finding by Delpy *et al.* (2008) of a hyperpolarized reversal potential of chloride in neonatal mouse MNs, there are two non-exclusive explanations for the increase in vestibular-mediated Ca^{2+} responses in MNs after blockade of GABA_A receptors: (1) bicuculline and PTX block GABA_A -mediated inhibition directly on MNs and thereby increase MN excitability and/or (2) bicuculline and PTX block GABA_A -mediated inhibition onto inhibitory interneurons and thereby disinhibit MNs. Both would produce the observed increase in vestibular-mediated Ca^{2+} responses in MNs. We cannot favour one possibility over the other until we characterize the relative distribution of GABA hyperpolarizing actions on MNs, excitatory interneurons and inhibitory interneurons.

Comparing the segment- and tract-specific organization of vestibulospinal inputs in newborn and adult mammals

We demonstrate a functional organization of vestibulospinal connections to spinal MNs in which most inputs to cervical segments are derived from the MVSTs whereas inputs to thoracic and lumbar segments are derived from the LVST (Fig. 10). A significant advance is a separate description of inputs deriving from the distinct iMVST and cMVST groups (Glover & Petrusdottir, 1988; Glover, 2000a; Pasqualetti *et al.* 2007), which have not been recognized as separate neuron populations in previous functional studies. We compare here the neonatal and adult patterns in more detail in the cervical, thoracic and lumbar segments separately.

In the upper cervical cord (C2 segment), inputs to the iMMC and cMMC derive, respectively, from the iMVST and cMVST. This is also the case in C6 except that in this segment inputs to iMMC derive from both the iMVST and the LVST. In addition, inputs to the iLMC derive solely from the LVST. Thus, at cervical levels, inputs from the LVST are only to the ipsilateral side and all inputs to the contralateral side derive from the cMVST. The pattern remains unchanged after midline lesions, indicating that vestibular activation of cervical MNs, which innervate neck, shoulder, trunk, forelimb and diaphragm muscles (Smith & Hollyday, 1983; Scarisbrick *et al.* 1990; McKenna *et al.* 2000 and references therein), is largely mediated by vestibulospinal axons without crossing collaterals and without intervening excitatory commissural interneurons. This pattern is in agreement with that reported in adult

mammals, where ipsilateral axial MNs in lower cervical segments receive inputs from both the LVST and the MVST, ipsilateral forelimb MNs receive inputs from the LVST alone, and contralateral MNs receive inputs from the MVST (cats: Wilson *et al.* 1995; Shinoda *et al.* 2006; rabbits: Akaike *et al.* 1973). The neonatal and adult patterns are therefore similar in the cervical segments except for the LVST-mediated excitation of axial MNs in rostral segments not seen in the neonate.

In T7 of the neonatal mouse, LVST axons provide inputs to both ipsi- and contralateral MMCs, with the latter inputs mediated either by locally crossing axon collaterals, excitatory commissural interneurons, or potentially by midline-crossing motoneuron dendrites. In adult cats (Wilson *et al.* 1970; T1–T10) and rabbits (Akaike *et al.* 1973; T2–T5), excitatory inputs to ipsilateral thoracic MNs have been reported to derive from the LVST and perhaps also the MVST. Some excitatory responses in contralateral MNs were also reported in adult rabbits but the source was not determined. Our findings in the neonatal mouse provide unequivocal demonstration of LVST-mediated inputs to both ipsilateral and contralateral thoracic MNs.

Inputs to MNs in lumbar segments in the neonatal mouse derive solely from the LVST, as is the case in adult mammals (Wilson & Yoshida, 1969), and inputs to contralateral MNs depend on intact commissures. Preliminary experiments in our lab have shown that commissural interneurons in L2 receive ipsilateral vestibulospinal inputs in the neonatal mouse and could therefore contribute to the commissure-dependent LVST-mediated responses in contralateral MNs (Perreault *et al.* 2009). Of particular interest is the finding that in contrast to the cervical and thoracic segments, there are no detectable vestibulospinal inputs to ipsilateral MMC MNs, either in L2 or L5, despite the fact that in both segments contralateral MMC MNs do receive inputs (Fig. 10). Vestibulospinal inputs to the lumbar MMC have not been investigated previously in adult mammals, but should be, given this intriguing laterality in the neonatal mouse.

Contribution from reticulospinal neurons

In rats, reticulospinal neurons are generated early during brain development (Altman & Bayer, 1980a,b; Bélanger *et al.* 1997) and are among the first to project axons to the spinal cord (Auclair *et al.* 1993, 1999; Easter *et al.* 1993; de Boer van Huizen & ten Donkelaar, 1999). Their axons extend into the lower thoracic and lumbar segments several days before birth (Kudo *et al.* 1993; Lakke, 1997). We have recently shown that reticulospinal projections in the neonatal mouse can activate lumbar motoneurons and interneurons (Szokol *et al.* 2008; Szokol & Perreault, 2009). Indirect activation of reticulospinal neurons by vestibular afferents occurs in adult mammals (Peterson

& Felpel, 1971; Peterson *et al.* 1980) but has yet to be demonstrated in neonates. Ongoing experiments in our laboratory are aimed at examining interactions between reticulospinal and vestibulospinal systems. In the present study we examined the possibility that reticulospinal pathways might contribute to vestibular nerve-mediated responses by performing extensive transverse lesions at the level of the brainstem. These lesions interrupted bilaterally all medially descending projections (including the MVST projections, projections from the pontine reticulospinal neurons and projections from medially located medullary reticulospinal neurons), sparing laterally descending projections including the LVST projection and projections from laterally located medullary reticulospinal neurons. These lesions greatly reduced but did not abolish the ipsilateral responses in C6 and T7 and had no effect on the ipsilateral responses in L2. The fact that, unlike stimulation of the VIIIth nerve, direct stimulation of the laterally located medullary reticulospinal neurons elicit Ca^{2+} responses in the iMMC of L2 (Szokol *et al.* 2008), leads us to suggest that the remaining responses seen after the brainstem lesions are likely to be mediated by the LVST rather than by the laterally located medullary reticulospinal neurons. Substantiation of this hypothesis will require further experimentation.

Dual component responses and mixed excitation/inhibition

LVST-mediated responses in lumbar iLMC MNs are dual-component, with the second component occurring after the end of the stimulus train (particularly obvious in L2). Since blockade of GABA_A receptors by bicuculline and PTX substantially increases the magnitude of both components, the inputs mediating these components are clearly mixed excitatory and inhibitory. Dual-component responses were never observed in contralateral MNs (see Fig. 8), suggesting that responses in ipsi- and contralateral MNs are mediated by different combinations of pathways with less convergence on the contralateral side. In adult mammals the LVST supplies excitatory or mixed excitatory/inhibitory inputs to LMC MNs in ipsilateral and contralateral lumbar segments (Shapovalov *et al.* 1966; Lund & Pompeiano, 1968; Wilson & Yoshida, 1969; Grillner *et al.* 1970; Hongo *et al.* 1971, 1975). Lumbar lamina VIII interneurons, which include inhibitory and excitatory commissural interneurons (most probably also in the neonate, see Restrepo *et al.* 2009), have been shown to be activated by LVST inputs in adult mammals, in parallel with activation of MNs (Aoyama *et al.* 1971; Skinner & Remmel, 1978; Grillner & Hongo, 1972; Krutki *et al.* 2003). In future experiments we intend to further characterize the monosynaptic and polysynaptic excitatory and inhibitory components of the

vestibulospinal responses using a combination of optical and patch clamp recording.

Functional considerations

Irrespective of the mono- or polysynaptic nature of the vestibulospinal connections to MNs, the segmental and tract-specific pattern reported in this study is based on the largest sample of MNs ever recorded from in a single study (>2000). The account nevertheless remains partial because it does not distinguish among responses elicited by activation of the different vestibular end-organs nor does it provide a complete picture of the inhibitory synaptic connections. These aspects will receive focus in future experiments. Despite these shortcomings we can conclude that in the neonate as in the adult the MVSTs exercise the principal control over cervical-innervated axial musculature whereas the LVST does so over limb musculature and thoracolumbar-innervated axial musculature. Thus, vestibular-mediated coordination of axial and forelimb muscles may be shared by the MVSTs and the LVST, suggesting that both pathways participate in motor behaviours that have been observed in rodents immediately after birth, including head movements, pivoting and righting reflexes (newborn rat; Clarac *et al.* 1998 and Lelard *et al.* 2006 and references therein; newborn mouse: our own unpublished observations). In contrast, the vestibular-mediated coordination of axial and hindlimb muscles is clearly the sole responsibility of the LVST. Of particular interest is the selective innervation of contralateral *versus* ipsilateral lumbar MMC MNs by the LVST. It seems likely that this is related to trunk stabilization coordinated to selective hindlimb movements, for example during single limb planting or lifting or during alternating limb movements. To summarize, the segmental and tract-specific connectivity pattern reported here is likely to be sufficient for sustaining an efficient postural stabilization at birth.

Conclusions

Functional excitatory synaptic connections are clearly established in the vestibulospinal pathways by birth in the mouse and exhibit many segment- and tract-specific features of the adult mammalian pattern. Obviously many aspects of connective organization may differ between neonate and adult, such as the degree of mono- and polysynapticity, the actual patterns of intervening interneurons, the numbers and distribution of synapses on target neuron dendritic arbors, the relative synaptic strengths, the presence of heterosynaptic interactions, and the degree of synaptic plasticity. The fact nevertheless remains that the overall pattern of segmental targeting seen in the neonate for neck and limb MNs

is remarkably similar to that previously described in the adult. The developmental mechanisms that underlie this pattern, including the differential longitudinal growth of iMVST, cMVST and LVST axons and their targeting to ipsilateral *versus* contralateral MN populations, must provide appropriate specificity very soon after, if not as, the axons reach the cord. Thus, as has been shown for the monosynaptic stretch reflex (Chen *et al.* 2003) and the vestibulo-ocular reflex (J. C. Glover, H. Mochida, K. Sato and Y. Momose-Sato, unpublished observations), a basic blueprint for adult connections appears to be predetermined already in the fetus. Moreover, the fact that vestibulospinal drive to axial MNs, which has not been assessed to the same extent in the adult, also shows a clear segmental and ipsi/contralateral specificity in the neonate indicates that these connections are also established selectively at early stages of development.

By this we do not imply that vestibulospinal connections to MNs and intervening interneurons are not refined postnatally, since the speed and amplitude of the descending connections increase progressively and motor patterns clearly are modified during the first weeks after birth (Clarac *et al.* 1998; Vinay *et al.* 2005). Nevertheless, our results indicate that postnatal motor refinement need not imply the presence of initially *inappropriate* connections. We would suggest that in the context of vestibulospinal control, postnatal refinement most probably occurs through the modulation of existing appropriate connections by later-developing sensory and descending inputs (Brocard *et al.* 1999, 2003; Vinay *et al.* 2000*b*) and through changes in the excitability of spinal neurons (Vinay *et al.* 2000*a*).

References

- Akaike T, Fanardjian VV, Ito M & Ono T (1973). Electrophysiological analysis of the vestibulospinal reflex pathway of rabbit. II. Synaptic actions upon spinal neurones. *Exp Brain Res* **17**, 497–515.
- Altman J & Bayer SA (1980*a*). Development of the brain stem in the rat. II. Thymidine-radiographic study of the time of origin of neurons of the upper medulla, excluding the vestibular and auditory nuclei. *J Comp Neurol* **194**, 37–56.
- Altman J & Bayer SA (1980*b*). Development of the brain stem in the rat. IV. Thymidine-radiographic study of the time of origin of neurons in the pontine region. *J Comp Neurol* **194**, 905–929.
- Aoyama M, Hongo T, Kudo N & Tanaka R (1971). Convergent effects from bilateral vestibulospinal tracts on spinal interneurons. *Brain Res* **35**, 250–253.
- Auclair F, Bélanger MC & Marchand R (1993). Ontogenetic study of early brain stem projections to the spinal cord in the rat. *Brain Res Bull* **30**, 281–289.
- Auclair F, Marchand R & Glover JC (1999). Regional patterning of reticulospinal and vestibulospinal neurons in the hindbrain of mouse and rat embryos. *J Comp Neurol* **411**, 288–300.
- Bélanger MC, Auclair F, Bertrand L & Marchand R (1997). The early neuronal organization predicts the path followed by some major axonal bundles in the embryonic brainstem. *Neuroscience* **78**, 259–270.
- Brocard F, Clarac F & Vinay L (2003). Gravity influences the development of inputs from the brain to lumbar motoneurons in the rat. *Neuroreport* **14**, 1697–1700.
- Brocard F, Vinay L & Clarac F (1999). Gradual development of the ventral funiculus input to lumbar motoneurons in the neonatal rat. *Neuroscience* **90**, 1543–1554.
- Bussi eres N, Pflieger JF & Dubuc R (1999). Anatomical study of vestibulospinal neurons in lampreys. *J Comp Neurol* **407**, 512–526.
- Buisseret-Delmas C, Compoin C, Delfini C & Buisseret P (1999). Organisation of reciprocal connections between trigeminal and vestibular nuclei in the rat. *J Comp Neurol* **409**, 153–168.
- Chen HH, Hippenmeyer S, Arber S & Frank E (2003). Development of the monosynaptic stretch reflex circuit. *Curr Opin Neurobiol* **13**, 96–102.
- Clarac F, Vinay L, Cazalets JR, Fady JC & Jamon M (1998). Role of gravity in the development of posture and locomotion in the neonatal rat. *Brain Res Brain Res Rev* **28**, 35–43.
- de Boer-van Huizen RT & ten Donkelaar JH (1999). Early development of descending supraspinal pathways: a tracing study in fixed and isolated rat embryos. *Anat Embryol* **199**, 539–547.
- Delpy A, Allain AE, Meyrand P & Branchereau P (2008). NKCC1 cotransporter inactivation underlies embryonic development of chloride-mediated inhibition in mouse spinal motoneuron. *J Physiol* **586**, 1059–1075.
- D az C & Glover JC (2002). Comparative aspects of the hodological organization of the vestibular nuclear complex and related neuron populations. *Brain Res Bull* **57**, 307–312.
- D az C, Glover JC, Puelles L & Bjaalie J (2003). The relationship between hodological and cytoarchitectonic organization in the vestibular complex of the 11-day chicken embryo. *J Comp Neurol* **457**, 87–105.
- Easter SS Jr, Ross LS & Frankfurter A (1993). Initial tract formation in the mouse brain. *J Neurosci* **13**, 285–299.
- Floeter MK & Lev-Tov A (1993). Excitation of lumbar motoneurons by the medial longitudinal fasciculus in the *in vitro* brain stem spinal cord preparation of the neonatal rat. *J Neurophysiol* **70**, 2241–2250.
- Glover JC (1995). Retrograde and anterograde axonal tracing with fluorescent dextran-amines in the embryonic nervous system. *Neurosci Prot* **30**, 1–13.
- Glover JC (2000*a*). Neuroepithelial ‘compartments’ and the specification of vestibular projections. *Prog Brain Res* **124**, 3–21.
- Glover JC (2000*b*). Development of specific connectivity between premotor neurons and motoneurons in the brain stem and spinal cord. *Physiol Rev* **80**, 615–647.
- Glover JC & Petursdottir G (1988). Pathway specificity of reticulospinal and vestibulospinal projections in the 11-day chicken embryo. *J Comp Neurol* **270**, 25–38.
- Grillner S & Hongo T (1972). Vestibulospinal effects on motoneurons and interneurons in the lumbosacral cord. *Prog Brain Res* **37**, 243–262.

- Grillner S, Hongo T & Lund S (1970). The vestibulospinal tract. Effects on α -motoneurons in the lumbosacral spinal cord in the cat. *Exp Brain Res* **10**, 94–120.
- Hongo T, Kudo N & Tanaka R (1971). Effects from the vestibulospinal tract on the contralateral hindlimb motoneurons in the cat. *Brain Res* **31**, 220–223.
- Hongo T, Kudo N & Tanaka R (1975). The vestibulospinal tract: crossed and uncrossed effects on hindlimb motoneurons in the cat. *Exp Brain Res* **24**, 37–55.
- Juvin L & Morin D (2005). Descending respiratory polysynaptic inputs to cervical and thoracic motoneurons diminish during early postnatal maturation in rat spinal cord. *Eur J Neurosci* **21**, 808–813.
- Kaada BR (1950). Site of action of myanesin in the central nervous system. *J Neurophysiol* **13**, 89–104.
- Karhunen E (1973). Postnatal development of the lateral vestibular nucleus (Deiters' nucleus) of the rat. A light and electron microscopic study. *Acta Otolaryngol Suppl* **313**, 1–87.
- Kasumacic N, Glover JC & Perreault MC (2008). Vestibulospinal drive to cervical and lumbar motoneurons investigated with calcium imaging in the neonatal mouse. *2008 Abstract Viewer/Itinerary Planner*, Programme No. 576.2. Society for Neuroscience., Washington, DC.
- Kasumacic N, Glover JC & Perreault MC (2010). Functional organization of vestibulospinal inputs to spinal motoneurons investigated with calcium imaging in the neonatal mouse. *Cellular and network functions in the spinal cord, Madison, Wisconsin 2009*.
- Krutki P, Jankowska E & Edgley SA (2003). Are crossed actions of reticulospinal and vestibulospinal neurons on feline motoneurons mediated by the same or separate commissural neurons? *J Neurosci* **23**, 8041–8050.
- Kudo N, Furukawa F & Okado N (1993). Development of descending fibers to the rat embryonic spinal cord. *Neurosci Res* **16**, 131–141.
- Lakke EA (1997). The projections to the spinal cord of the rat during development: a timetable of descent. *Adv Anat Embryol Cell Biol* **135**, 1–143.
- Lannou J, Precht W & Cazin L (1979). The postnatal development of functional properties of central vestibular neurons in the rat. *Brain Res* **175**, 219–232.
- Leong SK, Shieh JY & Wong WC (1984). Localizing spinal-cord-projecting neurons in neonatal and immature albino rats. *J Comp Neurol* **228**, 18–23.
- Lelard T, Jamon M, Gasc JP & Vidal PP (2006). Postural development in rats. *Exp Neurol* **202**, 112–124.
- Lev-Tov A & O'Donovan MJ (1995). Calcium imaging of motoneuron activity in the en-bloc spinal cord preparation of the neonatal rat. *J Neurophysiol* **74**, 1324–1334.
- Lev-Tov A & Pinco M (1992). *In vitro* studies of prolonged synaptic depression in the neonatal rat spinal cord. *J Physiol* **447**, 149–169.
- Lund S & Pompeiano O (1968). Monosynaptic excitation of α motoneurons from supraspinal structures in the cat. *Acta Physiol Scand* **73**, 1–21.
- McCluskey SU, Marotte LR & Ashwell KW (2008). Development of the vestibular apparatus and central vestibular connections in a wallaby (*Macropus eugenii*). *Brain Behav Evol* **71**, 271–286.
- McKenna JE, Prusky GT & Whishaw IQ (2000). Cervical motoneuron topography reflects the proximodistal organization of muscles and movements of the rat forelimb: a retrograde carbocyanine dye analysis. *J Comp Neurol* **419**, 286–296.
- Maklad A, Kamel S, Wong E & Fritzsche B (2010). Development and organization of polarity-specific segregation of primary vestibular afferent fibers in mice. *Cell Tissue Res* **340**, 303–321.
- Mbiene JP, Favre D & Sans A (1988). Early innervation and differentiation of hair cells in the vestibular epithelia of mouse embryos: SEM and TEM study. *Anat Embryol* **177**, 331–240.
- Morris RJ, Beech JN & Heizmann CW (1988). Two distinct phases and mechanisms of axonal growth shown by primary vestibular fibres in the brain, demonstrated by parvalbumin immunohistochemistry. *Neuroscience* **27**, 571–596.
- O'Donovan MJ, Ho S, Sholomenko G & Yee W (1993). Real-time imaging of neurons retrogradely and anterogradely labelled with calcium-sensitive dyes. *J Neurosci Methods* **46**, 91–106.
- Pasqualetti M, Díaz C, Renaud JS, Rijli FM & Glover JC (2007). Fate-mapping the mammalian hindbrain: segmental origins of vestibular projection neurons assessed using rhombomere-specific Hoxa2 enhancer elements in the mouse embryo. *J Neurosci* **27**, 9670–9681.
- Paxinos G, Halliday G, Watson C, Koutcherov Y & Wang HQ (2007). *Atlas of the Developing Mouse Brain at E17.5, P0, and P6*. Academic Press, Elsevier.
- Perreault MC, Kasumacic N, Glover JC & Szokol K (2009). Bulbospinal control of lumbar motor networks in the neonatal mouse (abstract). *Breathe, Walk and Chew: The Neural Challenge 31st Annual Symposium, Montreal*.
- Peterson BW (2004). Current approaches and future directions to understanding control of head movement. *Prog Brain Res* **143**, 369–381.
- Peterson BW & Felpel LP (1971). Excitation and inhibition of reticulospinal neurons by vestibular, cortical and cutaneous stimulation. *Brain Res* **27**, 373–376.
- Peterson BW, Fukushima K, Hirai N, Schor RH & Wilson VJ (1980). Responses of vestibulospinal and reticulospinal neurons to sinusoidal vestibular stimulation. *J Neurophysiol* **43**, 1236–1250.
- Pflieger JF & Cabana T (1996). The vestibular primary afferents and the vestibulospinal projections in the developing and adult opossum, *Monodelphis domestica*. *Anat Embryol* **194**, 75–88.
- Pflieger JF, Clarac F & Vinay L (2002). Picrotoxin and bicuculline have different effects on lumbar spinal networks and motoneurons in the neonatal rat. *Brain Res* **935**, 81–86.
- Restrepo CE, Lundfald L, Szabó G, Erdélyi F, Zeilhofer HU, Glover JC & Kiehn O (2009). Transmitter-phenotypes of commissural interneurons in the lumbar spinal cord of newborn mice. *J Comp Neurol* **517**, 177–192.

- Ruben RJ (1967). Development of the inner ear of the mouse: a radioautographic study of terminal mitoses. *Acta Otolaryngol* **220**, 1–44.
- Scarlsbrick IA, Haase P & Hrycyshyn AW (1990). The arrangement of forearm motoneurons in young and adult rats and the possibility of naturally occurring motoneuron death. *J Anat* **171**, 57–67.
- Shapovalov AI, Kurchavyi GG & Smrogonova MP (1966). Synaptic mechanisms of vestibulo-spinal influences on α -motoneurons (in Russian). *Fiziol Zh SSSR Im I M Sechenova* **52**, 1401–1408.
- Sher AE (1971). The embryonic and postnatal development of the inner ear of the mouse. *Acta Otolaryngol Suppl* **285**, 1–77.
- Sheykhohleslami K, Megerian CA & Zheng QY (2009). Vestibular evoked myogenic potentials in normal mice and Phex mice with spontaneous endolymphatic hydrops. *Otol Neurotol* **30**, 535–544.
- Shinoda Y, Sugiuchi Y, Izawa Y & Hata Y (2006). Long descending motor tract axons and their control of neck and axial muscles. *Prog Brain Res* **151**, 527–563.
- Skinner RD & Remmel RS (1978). Monosynaptic inputs to lumbar interneurons from the lateral vestibulospinal tract and the medial longitudinal fasciculus. *Neurosci Lett* **10**, 259–264.
- Smith CL & Hollyday M (1983). The development and postnatal organization of motor nuclei in the rat thoracic spinal cord. *J Comp Neurol* **220**, 16–28.
- Szokol K, Glover JC & Perreault MC (2008). Differential origin of reticulospinal drive to motoneurons innervating trunk and hindlimb muscles in the mouse revealed by optical recording. *J Physiol* **586**, 5259–5276.
- Szokol K & Perreault MC (2009). Imaging synaptically mediated responses produced by brainstem inputs onto identified spinal neurons in the neonatal mouse. *J Neurosci Methods* **180**, 1–8.
- Tanaka Y, Tanaka Y, Furuta T, Yanagawa Y & Kaneko T (2008). The effects of cutting solutions on the viability of GABAergic interneurons in cerebral cortical slices of adult mice. *J Neurosci Methods* **171**, 118–125.
- Takemura K & King WM (2005). Vestibulo-collic reflex (VCR) in mice. *Exp Brain Res* **167**, 103–107.
- Van De Water TR, Wersäll J, Anniko M & Nordeman H (1978). Development of the sensory receptor cells in the utricular macula. *Otolaryngology* **86**, 297–304.
- van Mier P & ten Donkelaar HJ (1984). Early development of descending pathways from the brain stem to the spinal cord in *Xenopus laevis*. *Anat Embryol* **170**, 295–306.
- Vinay L, Cazalets JR & Clarac F (1995). Evidence for the existence of a functional polysynaptic pathway from trigeminal afferents to lumbar motoneurons in the neonatal rat. *Eur J Neurosci* **7**, 143–51.
- Vinay L, Ben-Mabrouk F, Brocard F, Clarac F, Jean-Xavier C, Pearlstein E & Pflieger JF (2005). Perinatal development of the motor systems involved in postural control. *Neural Plast* **12**, 131–139.
- Vinay L, Brocard F & Clarac F (2000a). Differential maturation of motoneurons innervating ankle flexor and extensor muscles in the neonatal rat. *Eur J Neurosci* **12**, 4562–4566.
- Vinay L, Brocard F, Pflieger JF, Simeoni-Alias J & Clarac F (2000b). Perinatal development of lumbar motoneurons and their inputs in the rat. *Brain Res Bull* **53**, 635–647.
- Wilson VJ, Boyle R, Fukushima K, Rose PK, Shinoda Y, Sugiuchi Y & Uchino Y (1995). The vestibulocollic reflex. *J Vestib Res* **5**, 147–170.
- Wilson VJ & Peterson BW (1978). Peripheral and central substrates of vestibulospinal reflexes. *Physiol Rev* **58**, 80–105.
- Wilson VJ & Yoshida M (1969). Comparison of effects of stimulation of Deiters' nucleus and medial longitudinal fasciculus on neck, forelimb, and hindlimb motoneurons. *J Neurophysiol* **32**, 743–758.
- Wilson VJ, Yoshida M & Schor RH (1970). Supraspinal monosynaptic excitation and inhibition of thoracic back motoneurons. *Exp Brain Res* **11**, 282–295.
- Ye JH, Zhang J, Xiao C & Kong JQ (2006). Patch-clamp studies in the CNS illustrate a simple new method for obtaining viable neurons in rat brain slices: glycerol replacement of NaCl protects CNS neurons. *J Neurosci Methods* **158**, 251–259.
- Zelenin PV, Pavlova EL, Grillner S, Orlovsky GN & Deliagina TG (2003). Comparison of the motor effects of individual vestibulo- and reticulospinal neurons on dorsal and ventral myotomes in lamprey. *J Neurophysiol* **90**, 3161–3167.
- Ziskind-Conhaim L (1990). NMDA receptors mediate poly- and monosynaptic potentials in motoneurons of rat embryos. *J Neurosci* **10**, 125–135.

Author contributions

All authors approved the final version of the manuscript for publication. J.C.G. and M.-C.P. conceived and designed the experiments; N.K. performed the experiments and analysed the data; N.K., J.C.G. and M.-C.P. drafted the manuscript.

Acknowledgments

We are grateful to Kobra Sultani and Marian Berge Andersen for technical assistance. This work was supported by grants from the Medical Faculty of the University of Oslo and the Norwegian Research Council to M.-C.P. and J.C.G. and a grant from the International Foundation for Research in Paraplegia to M.-C.P.